



**VICTORIA UNIVERSITY**  
MELBOURNE AUSTRALIA

*The fabrication and surface functionalization of porous metal frameworks – a review*

This is the Accepted version of the following publication

Dumee, Ludovic, He, Li, Lin, Bao, Ailloux, Francois-Marie, Lemoine, Jean-Baptiste, Velleman, Leonora, She, Fenghua, Duke, Mikel, Orbell, John, Erskine, Gilbert, Hodgson, Peter, Gray, Stephen and Kong, Lingxue (2013) The fabrication and surface functionalization of porous metal frameworks – a review. *Journal of Materials Chemistry A*, 1 (48). pp. 15185-15206. ISSN 2050-7496

The publisher's official version can be found at  
<http://pubs.rsc.org/en/content/articlelanding/2013/ta/c3ta13240d#!divAbstract>  
Note that access to this version may require subscription.

Downloaded from VU Research Repository <https://vuir.vu.edu.au/24461/>

# The fabrication and surface functionalization of porous metal frameworks – a Review

## Authors

Ludovic F. Dumée<sup>1,2\*</sup>, Li He<sup>1</sup>, Bao Lin<sup>1</sup>, Francois-Marie Allioux<sup>1,3</sup>, Jean-Baptiste Lemoine<sup>1,3</sup>, Leonora Velleman<sup>1</sup>, Fenghua She<sup>1</sup>, Mikel C. Duke<sup>2</sup>, John D. Orbell<sup>2</sup>, Gilbert Erskine<sup>4</sup>, Peter Hodgson<sup>1</sup>, Stephen Gray<sup>2</sup>, Lingxue Kong<sup>1</sup>

1 Institute for Frontier Materials – Deakin University, Piggons Road, Waurn Ponds 3216, Victoria – Australia

2 Institute for Sustainability and Innovation, College of Engineering and Science, Victoria University, Hoppers Lane, Werribee 3030, Victoria – Australia

3 Université Paul Sabatier III, Route de Narbonne, Toulouse 31062 - France

4 Advanced Metallurgical Solutions, Lonsdale 5160, South Australia - Australia

\* Corresponding author: [ludovic.dumee@deakin.edu.au](mailto:ludovic.dumee@deakin.edu.au); +61410131312

## **Abstract**

Porous metal frameworks offer potentially useful applications for the aerospace, automotive and bio-medical industries. They can be used as electrodes, actuators, or as selective membrane films. The versatility of the physical features (pore size, pore depth, overall porosity and pore surface coverage) as well as the large range of surface chemistries for both metal oxides and pure noble metals offers scope to functionalise metal nano-particles and networks of nano-porous metal structures. As well as traditional routes to producing metal structures, such as metal sintering or foaming, novel high-throughput techniques have recently been investigated. Nanoparticle self-assembly, metal ion reduction and deposition as well as metal alloy de-alloying were identified as sustainable routes to produce large surface areas of such nano-porous metal frameworks. The main limitations of the current fabrication techniques include the difficulty to process stable and homogeneous arrays of nano-scale pores and the control of their morphology due to the high reactivity of nano-structured metal structures. This paper aims at critically reviewing the various fabrication techniques and surface functionalization routes used to produce advanced functional porous metal frameworks. The limitations and advantages of the different fabrication techniques will be discussed in light of the final material properties and targeted applications.

## **Keywords**

porous metal frameworks; porous metal fabrication routes; metal surface chemistry; application of metal frameworks;

## **TABLE OF CONTENTS**

### **1. Introduction**

### **2. Fabrication techniques of porous metal frameworks**

2.1 Chemical vapour deposition

2.2 Deposition from liquid metal

2.3 Solid phase forming

2.4 Metal ions deposition and assemblies

2.5 Nanoparticle preparation and assemblies

2.6 De-alloying

2.7 Properties and morphology of porous metal structures

### **3. Chemistry of metal surfaces**

3.1 Metal oxides

3.2 Pure metal

3.3 Summary

### **4. Major fields of application of porous metal frameworks**

4.1 Heat storage and dissipation

4.2 Reinforcement for composite materials

4.3 Sensing

4.4 Orthopaedic and medical use

4.5 Membrane separation

### **5. Conclusion and prospects**

### **References**

## 1. Introduction

Porous metal materials, made from pure and alloyed metals or metal oxides, and exhibiting through-pores at the meso or macro scale, have been studied and used since the mid 1920's<sup>1</sup>. The scope of applications of porous metal frameworks includes separation membranes,<sup>2, 3</sup> conductive porous electrodes<sup>4-7</sup>, biocompatible scaffolds<sup>8, 9</sup>, sensing<sup>10-13</sup>, actuators<sup>14</sup> and hybrid composite materials<sup>15, 16</sup>. The development of porous cellular metal materials has been driven by the need for low density and high stiffness materials in the composite-material industry<sup>17-19</sup>. The morphology of the porous metal framework materials, i.e. the size and depth of the pores, overall porosity and pore surface coverage, may vary greatly with fabrication technique.

Metal foams have been used in the automotive, bio-medical, and aerospace industries for their superior mechanical and thermo-electrical conduction properties<sup>15, 17, 20-25</sup>. Metal foams and sponges show enhanced mechanical stability compared to their porous polymeric equivalents and have the advantages of both metallic characteristics and the soft matter properties found in polymers<sup>15, 18, 20</sup>. The morphology and inter-connectivity of cells across structures made of non-connected voids (as in foams) or semi-continuous and tortuous networks (as in sponges) allows for a very fine tuning of bulk material properties. Other porous metal structures, including cast<sup>26</sup> or electroplated metal grids or sintered particles, nanoparticles (NPs) or fibre meshes, have also been fabricated and commercialized and offer cheap and highly versatile pore structures that can be altered by changing the substrate geometry or the dimensions (size, length or aspect ratio), respectively<sup>27-30</sup>. The processing of either pure or alloyed porous metal structures has been demonstrated from noble metals, such as gold, palladium or platinum, as well as for copper, aluminium, nickel or iron, thereby offering a wide range of chemistries relevant to specific applications<sup>31</sup>. The recent interest in nano-textured metal surface chemistry has also opened new routes to the preparation of 'smart' functionalization of either metal oxide or pure metal surfaces<sup>32</sup>. In addition, recent research on innovative porous metal structure fabrication such as electro-less deposition<sup>33-35</sup>, block co-polymer self-assembly mixed with metal particles<sup>36-38</sup> and de-alloying<sup>39</sup>, has opened the way to exciting opportunities and applications for such porous metal frameworks. The development of innovative and inexpensive metal materials promises to benefit

both industry and the community in fields such as those that utilize abrasive liquid waste purification, industrial solvent mixtures, extremely concentrated brines or extreme pH conditions.

This article aims to critically review the various fabrication techniques and surface functionalization routes that have been demonstrated to date to successfully produce advanced functional porous metal frameworks. The advantages and limitations of these fabrication techniques will be discussed in light of the final material properties and the suggested/reported applications (sensing, biological scaffolds and separation). This review presents, for the first time, a critical analysis of the relationship between the fabrication routes and the morphology of the metal frameworks. The present article also aims at correlating the metal frameworks morphology to their properties and highlights the potential and importance of surface functionalization towards specific applications. The most promising approaches and future research directions to process and chemically functionalize nano and macro porous metal frameworks are identified and both advantages and limitations are discussed.

## 2. Fabrication techniques of porous metal frameworks

A number of techniques have been used to fabricate porous metal frameworks and foams and the five most widely used are: (i) bottom-up growth, (ii) top-down milling, (iii) phase removal, (iv) compaction / sintering, and (v) templating, Figure 1. Each of these general approaches has been translated into a variety of processes and the major techniques will be described and discussed in this section. Although the focus will be on porous metal structures made of pure metal or metal oxides, some composite and hybrid structures made of different layers, reinforcements or coatings of metals, organics or ceramics, will also be presented.

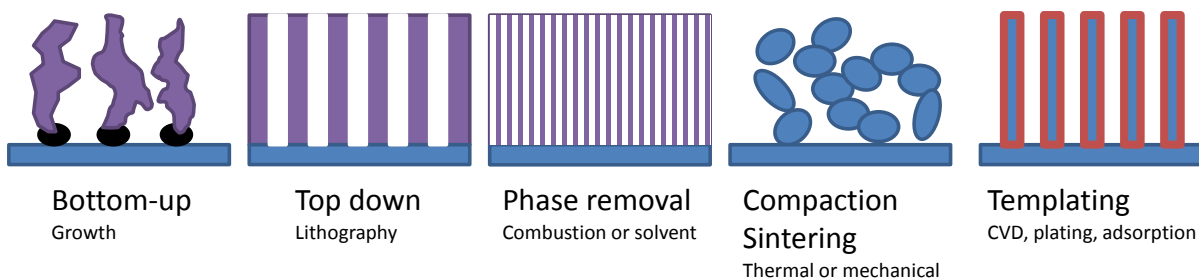


Figure 1 Schematic routes to processing porous metal frameworks

### 2.1 Metal chemical vapour deposition

Chemical vapour deposition (CVD) produces thin layers of metal on different substrates such as metals, ceramics or polymers<sup>40-43</sup>. This technique has the advantage of producing a thin imprint that perfectly follows the substrate's topography and morphology<sup>44</sup>. It is, however, typically only used to coat thin layers of pure metals, such as gold, platinum, palladium, zinc or nickel, onto the substrate in order to exploit the metal's electrical or thermal properties. Although CVD deposition is routinely used for the preparation of gas separation and H<sub>2</sub> permeable membranes<sup>45-47</sup>, a small number of porous metal/polymer composite and metal/ceramic membranes have been investigated for applications to continuous oxidation for water treatment<sup>48-52</sup>.

## 2.2 Deposition from liquid metal

### *2.2.1 Direct and investment casting*

The direct casting technique is typically applied for the production of large pore filters and grids. It is, however, not well suited to the fabrication of sub-micron pore size materials due to the difficulties associated with preparing the reciprocal imprint that is required for narrow pores. Membranes with arrays of well controlled and periodic pores can be obtained by this method. Although they are mostly used in gas purification, they also find applications in many industrial processes requiring very large particle removal or for membrane reactors or bio-reactors. The pores are typically of the order of hundreds of microns, thereby offering low liquid resistance but also low selectivity<sup>18, 23</sup>.

Investment casting uses an initial template, such as polymeric foam to define the structure of the final metal foam. The template foam is typically filled with a dense, heat resistant material such as a zeolite or phenolic resin, prior to being removed. The image of the template then remains in the structure. For example, carbonization and casting of molten metal leads to a replica of the initial template foam. The filler can then be removed to reveal the pure metal foam. This technique leads to very fine pore size foams, whose morphology directly relates to that of the template foam. Furthermore, light-weight metal foams can be fabricated in this way by casting around inorganic plain or hollow particles of low density, or by infiltrating a liquid melt through such a porous micron sized template<sup>18, 23</sup>. The major limitation of melt metal usage is therefore the limited interconnectivity of the pores within the metal matrix.

### *2.2.2 Direct gas foaming*

Gas injection for direct foaming within a molten liquid metal will also lead to a foam or sponge structure depending on the interconnectivity of the gas bubbles, the cooling and crystallization time, and on the temperature/viscosity of the liquid metal at the time of injection<sup>19</sup>. The pore morphology can be tuned by changing the gas type (such as N<sub>2</sub> or argon - air is also used), or the impeller gas pressure<sup>17</sup>. The foam typically forms at the surface of the metal melt and can be extracted through a conveyor belt, prior to cooling. Mechanical reinforcement of the melt can be adjusted

prior to foaming by adding silicon carbide (SiC) or alumina ( $\text{Al}_2\text{O}_3$ ). This is typically performed in order to reinforce the foam prior to cutting.

The theory of metal foaming directly relies on percolation and scaling theories<sup>53</sup>. Foams are considered as infinite networks of randomly distributed pores within a rigid matrix. The pore connectivity, size, density, as well as the nature and morphology of the rigid matrix may vary depending on the processing technique and materials used. The effective connectivity threshold, i.e. the ratio  $K/K_0$  as defined in Equation 1, follows a power-law function of the material's relative density<sup>18</sup>:

$$\frac{K}{K_0} = z \cdot \left( \frac{\rho}{\rho_0} \right)^t \quad (1)$$

where  $K$  and  $\rho$  are the effective connectivity and density of the foam respectively,  $K_0$  and  $\rho_0$  correspond to the properties of the rigid matrix composing the cell wall material and  $z$  and  $t$  are geometrical and physical constants, respectively. The effective connectivity is here an indication of tortuosity, relating to the minimum distance for a molecule to travel across the pores of the material. This value is always greater than 1; unity corresponds to straight-through pores.

### 2.2.3 Foaming agent injection

Similar to direct foaming, heating of a mixture of metal and a heat unstable foaming agent can lead to the formation of highly porous metal foams. Above the decomposition temperature, the foaming agent will decompose, thereby releasing gas, typically  $\text{CO}_2$ , which forms macro-cavities within the cooling metal structure. The type of foaming agent, and its decomposition temperature and reactivity will govern the gas bubble rate formation and the overall foam porosity (67 – 75 %)<sup>18</sup>. Nano-foams from sol-gel auto-combustion with pore sizes around 20 to 100 nm were also obtained through a similar technique, leading to a low density iron foam, Figure 2<sup>54</sup>.

Although gas bubble coalescence can lead to a continuous porous network, special conditions and foaming agents must be used to achieve reliable pore interconnectivity.

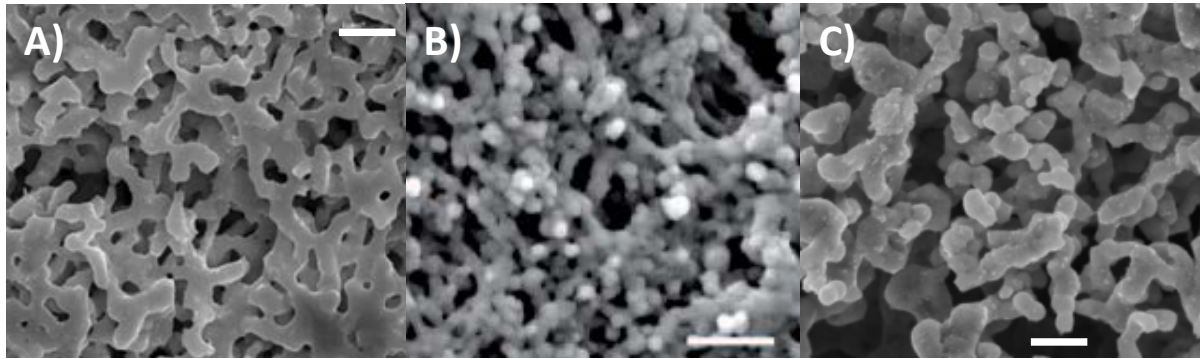


Figure 2 Examples of nano-foams, (a) silver (scale bar 1  $\mu\text{m}$ ), (b) titanium (scale bar 1  $\mu\text{m}$ ) and (c) nickel (scale bar 200 nm) from<sup>55</sup>

### 2.3 Solid phase forming

Porous metal materials can also be produced in the solid phase by processing metal powders and fibres. The most common technique to produce large volumes is thermo-mechanical sintering, but recent work has also demonstrated the benefits, in term of structure stability, of electrical sintering.

#### *2.3.1 Thermo-mechanical sintering*

A number of mechanical sintering techniques have been demonstrated to lead to porous metal structures, typically involving hot or cold compression of either a mesh of metal fibres or a bed of metal beads. Sample heating can be achieved through direct conduction, micro-waves or light-laser irradiation<sup>29, 56-59</sup>. The properties of the porous metal materials' compressibility and the required morphology of the final product will determine the most appropriate heating technique<sup>30</sup>. The size and reactivity of the particles to be sintered have to be well understood in order to avoid densification by over-heating and fusion<sup>28</sup>.

The major principle of sintering relies on the neck growth and direct mass transfer between particles that lead to their agglomeration<sup>60</sup>. The neck of a porous material structure is here defined as the average dimension of matter interconnecting two or more cavities. This is particularly critical with metal based structures due to the high degree of particle interconnection after sintering. The ratio of the neck size ( $x$ ) to the particle radius ( $r$ ) was demonstrated to depend on the sintering time ( $t$ ),

and a number of parameters related to the dominant sintering energy transfer mechanism ( $m$ ,  $n$  and  $F$ ) as shown in Equation 2<sup>27, 56</sup>:

$$\frac{x}{r} = \left( \frac{-F.t}{r^n} \right)^{1/m} \quad (2)$$

The average densification of the structure can be determined by calculating the average shrinkage of the centre-to-centre distance between particles where the centre to centre distance between particles is defined as ( $L$ ), following Equation 3<sup>61</sup>:

$$\frac{\Delta L}{L} = \left( \frac{-F.t}{2^m r^n} \right)^{2/m} \quad (3)$$

Pore formation relies on the remaining distance between the particles after sintering, and on the average particle deformation induced by the process. This technique can lead to higher pore interconnectivity than that with melt metal processes as described in Section 2.2.1. Although the kinetics of neck formation is well understood for large macro-particles, the sintering kinetics of NPs was demonstrated to be rapid due to their large specific surface area. This was attributed to the higher probability of defects or functional groups on the NPs surface, as well as to their enhanced thermal diffusivity arising from size effects and to the larger number of contacts made between NPs within agglomerates. Foaming agents, similar to the ones used in liquid forming, can also be added in order to enhance the porosity of the structure<sup>57, 62</sup>.

### 2.3.2 Electrical and chemical sintering

Electrical sintering of metal particles can be achieved by applying a current across a pre-formed agglomerate of particles in order to induce softening of the metal by heat dissipation - also called the Joule effect<sup>63, 64</sup>. This technique has been used particularly for the preparation of metal electrodes and conducting pathways for electronics as the electrodes can be moved across the agglomerate surface. This allows flexibility in the patterns and degree of sintering by changing the percolation threshold of the structure obtained. It was also reported to allow tuning of the metal grain size<sup>65</sup>.

The sintering of NPs has also been studied and has led to promising, highly porous structures. The altered surface morphology associated with NPs affects their properties and leads to, for example, lower melting points and electrical resistances, facilitating coalescence and decreasing the required energy for sintering. Silver NP (~50 nm) assemblies were sintered by low voltage (<10 V) and their coalescence behaviour was monitored in-situ with a Transmission Electron Microscope (TEM)<sup>66, 67</sup>. The coalescence kinetics was found to be very fast (of the order of hundreds of milli-seconds) depending on the applied voltage, and follows a two-step mechanism. Although metal neck formation by metal ion surface diffusion is found to be the starting point and the dominant factor in the formation of larger NPs, the speed of formation of larger NPs is sharply decreased due to the increase of the electrical resistance of these larger agglomerates. Although iso-porous and homogeneous materials are generally undesirable outcomes, the formation of controlled bottlenecks might lead to the fabrication of customized-shaped nano-pores, within the 10 to 100 nm range, and nano-compartments that could be favourable for applications such as molecular separation or gas storage<sup>68, 69</sup>. The development of hourglass pores, for example, is of great interest in mimicking charge and mass diffusion across the living cell gate-keepers, viz. aquaporin<sup>70, 71</sup>, or for drug delivery systems<sup>72</sup>. Hour-glass structure, based on two nano-compartments interconnected through a narrow neck pore, are able to enhance separation and selectivity through a motion kinetic gradient between the compartment and the neck. This morphology is typically found in porous metal frameworks prepared by sintering, on both nano and macro-porous scales due to the fusion of near-by particles.

Charge transfer sintering was demonstrated between silver NPs when exposed to an electrically active poly-electrolyte such as poly(di-allyl,di-methyl ammonium chloride) (PDAC)<sup>73</sup>. Densely packed arrays of NPs can be partially fused at room temperature to obtain larger interconnected aggregates, thus forming a highly porous network. This technique is applicable to the production of large surface areas, and for the processing of thick porous structures typically performed by ink-jet printing<sup>74, 75</sup>. The major limitation of this technique, however, resides in the preparation and stabilization of the ligands which may involve the use of surfactants or non-conductive fillers<sup>76</sup>.

Electrical arc spraying discharge onto stainless steel macro-particles was also demonstrated to lead to slightly porous structures. Although the porosity did not exceed 10 % for very large pores (10 – 50 µm), the large content of metal oxides present (up to 30%) could be used if appropriately reduced to generate large porosity materials<sup>77</sup>.

### *2.3.3 Composite powder mixture extrusion*

Powder extrusion was also demonstrated to fabricate micron sized pore - porous metal cellular foams and structures. Polymer-metal mixtures are used in industry to prepare high loading metal reinforced composites, which are then annealed to remove the polymer matrix<sup>78</sup>. This technique is highly versatile and allows for the preparation of materials with a variety of pore size distributions, ranging from a few hundreds of nano-meters up to a few dozen microns. The geometry of the pores and overall porosity is, however, limited by the sintered particles. Therefore the development of nano-porous frameworks requires the sintering of NPs, and due to their high surface to volume ratios, also requires the management of their resultant fast coalescence<sup>79</sup>. At high concentrations, metal NPs tend to aggregate into semi-dense clusters, unable to be properly dispersed within the hydrophilic phase of the block co-polymer (BCP) and thereby preventing the formation of ordered pores<sup>80</sup>. In addition, the high density of the metal NPs requires large volumes of particles to be added to the extrusion mixture, strongly increasing the viscosity of the dope<sup>81</sup>.

The porosity of these extruded materials is typically relatively low (below 50%) due to strong sintering and macro-particle fusion<sup>82, 83</sup>. Thus although being highly versatile and efficient for the production of flat sheet or fibrous porous materials, composite powder extrusion/carbonization is limited to a high pore range - towards the micron benchmark. The trade-off between the carbonization temperature of the sacrificial polymer and coalescence by sintering of the metal NPs is therefore the main difficulty to be overcome in order to achieve high porosity and nano-scale pore size membranes. Routes to stabilize the structures might however include the use of a highly viscous or a solid sacrificial phase that can be decomposed or evaporated at low temperature, followed by 'cold sintering' (up to 100°C); to simultaneously limit

coalescence and remove the sacrificial phase. Current research on the self-assembly and coalescence of metal NPs is directed towards room temperature or cold sintering in order to maintain the high surface area and catalytic properties of the metal NPs. Consequently, cold composite powder extrusion might become viable in the near future.

#### *2.3.4 Slurry foaming*

As opposed to direct metal foaming, slurry foaming involves two consecutive steps in order to form largely open cell foams. The interconnectivity of these foams is typically higher than that of foaming agent decomposition foams and pore sizes down to tens of micrometers were achieved. Slurry foaming operates on the basis of drying a mixture of a foaming agent (surfactant, polymer or volatile compound in a solvent) and a metal particle slurry that expands at elevated temperatures. As temperature rises, the viscosity of the slurry is increased and gas is released, thus leading to porous open cell metal foams. However, post-reduction and annealing of the structures is generally necessary, both to enhance the mechanical properties and to sinter the metal particles into a continuous network. Although porosities close to 93% have been achieved with aluminium powders, issues relating to crack formation and low mechanical stability, when compared to conventional foaming products, were reported to occur due to the poor linkage between the metal particles 22, 24, 84, 85.

Although the very high porosity of these materials would be of interest for flow-through contactors or membranes, the potential and great versatility of slurry foaming is limited by the formation of very large pores due to the sacrificial phase expansion process. These foams might however form very promising supports for composite multi-layer metal porous structures if judiciously combined with meso or nano-porous metal layers, or as electrically conducting plating substrates for electro or electro-less metal deposition.

## 2.4 Metal ion deposition, reduction or assemblies

### *2.4.1 Electro-plating*

Electro-plating has been used to coat surfaces including highly porous substrates for which the pores may be on the micron scale. The control of the technique within porous structures is challenging due to the requirement of using the surface as an electrode. This leads, within micro and nano-porous structures to pore filling and clogging<sup>86, 87</sup>. This substantially reduces the surface porosity and pore density. In electro-deposition, the substrate to be plated is used as an electrode in conjunction with a counter electrode. The metal ion feedstock can either be present within a solution, as a metal salt, or if high enough electrical currents are provided, may be generated from the oxidation of the metallic counter electrode. As the rate of deposition is directly related to the applied current across the plating cell, electro-plating is therefore a highly efficient method for the fast processing of rough coatings of metals. It is possible to prepare porous membranes of large pores with this technique, but the specificity of the support geometries and the relatively poor control of the porosity of the coating are generally not considered sufficient for membrane standards. Therefore, this method has not been extensively used for the preparation of porous metal membranes<sup>86</sup>.

Although not entirely suitable on its own, the application of electro-plating, as a cheap and fast binding technique, into mechanically weak pre-formed metal materials with large pore size, such as foams, may lead to reinforced materials with narrower pore size distributions. This may, however, dramatically reduce the final porosity of the material and lead to pore obstruction of either open or closed macro-compartments. Electro-plating may also be used to prepare cheap metal plated supporting layers for active layers prepared through other techniques. For example it is possible to plate ‘cheap’ metals, such as copper, aluminium or nickel onto preformed polymeric materials such as textile reinforcements or porous grids.

#### *2.4.2 Electroless deposition*

Electroless deposition, although exhibiting a much slower rate of deposition than electro-deposition, is a much more appropriate technique for the fabrication of porous metal substrates<sup>88, 89</sup>. Electroless deposition is generally a 3-step process, Figure 3, in which a metal is deposited from solution onto an activated surface. During the first step, referred to as sensitization, the surface is immersed in a solution of tin which can chelate with functional groups on the surface. In the second step, referred to as activation, the surface is typically immersed in a solution containing highly noble metal ions, such as silver or palladium, to deposit catalytic particles of a high density onto the surface. In the third step, the activated surface is immersed in a final metal plating bath containing a reducing agent (commonly formaldehyde, dimethylamine borane, hypophosphite). The catalytic silver or palladium particles adsorbed onto the surface provide sites for the reduction of the metal ions onto the surface, Figure 3.

The deposition mechanism occurs via the nucleation, growth and coalescence of metal particles onto the surface. The thickness of the deposited metal layer will increase with time and the process can be stopped when the desired thickness is reached. A number of highly porous and organized metal structures have been successfully prepared with electro-less deposition<sup>89</sup>. Electroless deposition presents a beneficial technique for the fabrication of highly controllable structures. It can coat surfaces within confined spaces such as porous materials and is not discriminative of the nature of the substrate material used. However electroless deposition of porous materials requires a high density of initial nucleation sites in order to form a highly compact and homogeneous metal coating. A higher density of nucleation sites can be achieved by adopting a slower rate of deposition that will allow enough time for the initial nuclei to form before the growth stage dominates. Additionally a controlled and slow deposition rate is required for the coating of porous membranes as the metal is preferentially deposited onto the top surfaces of the membrane. Therefore, a slower deposition rate will allow deposition to occur within the depths of the pores - before the pores at the surface of the membrane are blocked. The deposition rate is controlled by the pH, temperature, concentration of metal ions, reducing agents and complexing agents within the plating bath. Through altering the bath conditions the deposition rate can vary between a few nanometres to a few hundred microns an

hour. The versatility of electro-less deposition has allowed a number of porous substrates to be efficiently plated including polymer surfaces<sup>90-93</sup>, carbon fibres<sup>94</sup>, metal surfaces and particles<sup>34, 95</sup>, carbon nanotube surfaces<sup>96</sup>, glass<sup>97, 98</sup> or porous ceramics (silica, alumina, titania)<sup>35, 99-102</sup>. Gold and metal nanotube membranes have been fabricated through this approach and used for electrode fabrication<sup>103</sup>, molecular separation<sup>100, 104</sup>, lithography,<sup>105</sup> and sensing<sup>13, 106</sup>.

The simultaneous co-deposition of different metals was also demonstrated to be an effective way to produce porous or dense metal alloy layer<sup>107, 108</sup>. Although metal deposition is thermodynamically specific due to the affinity between the sensitizing agent and the metal ions, simultaneous metal deposition is possible through controlling the mixture of different sensitizing agents. The co-deposition rate is then proportional to the individual selective adsorption of the sensitizing agent and on their relative surface coverage on the substrate. This technique could prove to be a very powerful method for the preparation of finely tuned alloyed structures with nano-scale grain size for use in de-alloying or sintering metal particle mixtures.

The slow kinetics of electro-less deposition and the necessity for a chemically compatible and physically accessible surface are the main limiting factors in the development of porous metal structure fabrication. A trade-off between deposition rate and homogeneous coating must therefore be achieved, with higher deposition rates leading to coarser structures with larger grains and lower rates leading to smoother and denser deposition. The template materials need to possess either very specific properties, such as high wettability and preferential good affinity for the sensitizing agent, while also being highly porous - to allow for metal deposition<sup>109</sup>.

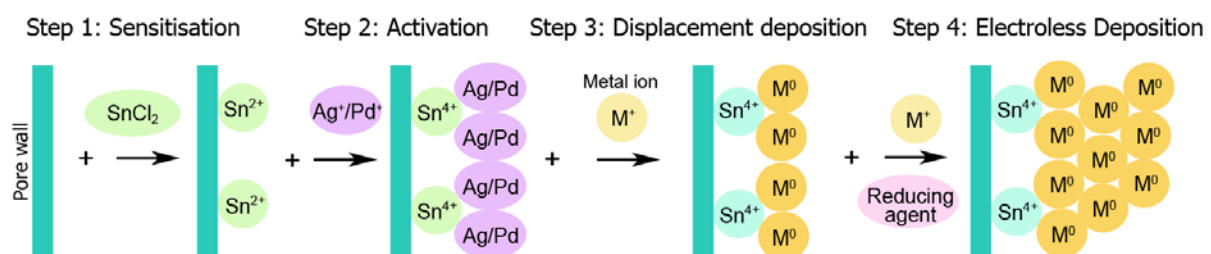


Figure 3 Electroless deposition plating procedure<sup>110</sup>

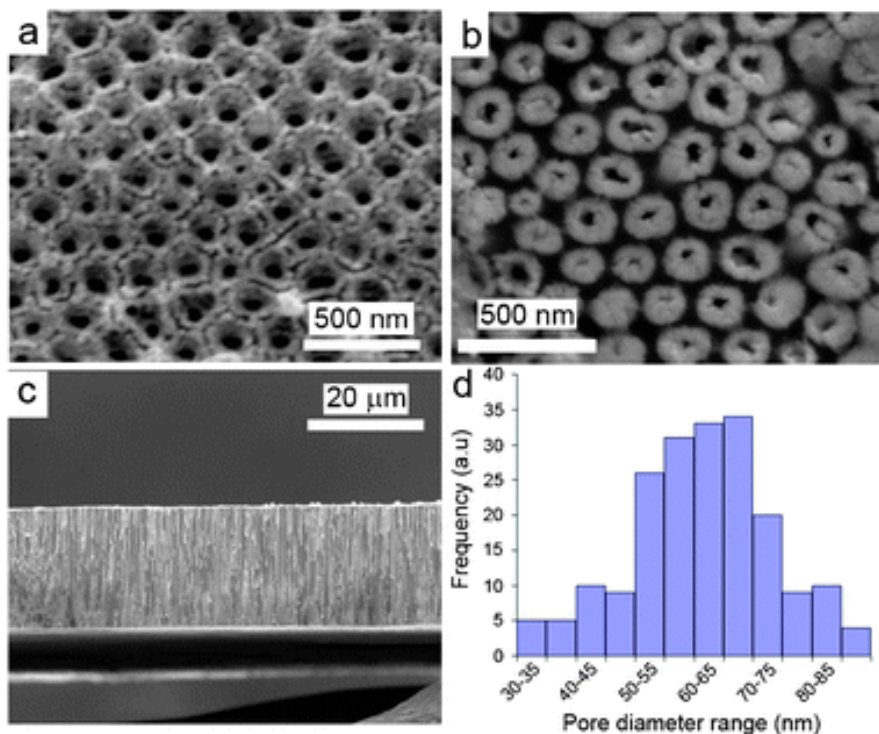


Figure 4 Example of gold electroless deposition onto a porous alumina template. (a) presents the alumina support prior to metal deposition, (b) the formation of the gold nanotubes across the alumina pores, (c) a cross section of the alumina after plating and (d) the pore size distribution determined from the SEM image (b)<sup>111</sup>

#### 2.4.3 Electro-spun web fabrication

Electro-spinning is a technique used to extrude and produce nano-fibres with a diameter ranging in the order of the tens to hundreds of nanometres. ES has been used to fabricate very thin polymeric<sup>112-114</sup>, ceramic<sup>115</sup> and metal fibres<sup>116, 117</sup>. Plain<sup>118, 119</sup>, hollow<sup>120</sup> and porous<sup>116, 121</sup> metal fibres have been prepared from metal salts mixed into dissolved polymer solutions. Electro-spinning was shown to be an excellent technique for producing ramified or branched fibrous materials<sup>122</sup>, and this has been applied to filtration methods since the early 2000<sup>123</sup>. A number of metal nano-fibres including indium<sup>124, 125</sup>, iron<sup>126</sup>, cobalt<sup>126</sup>, nickel<sup>127</sup>, and copper<sup>128</sup> have been produced by metal salt electro-spinning. During the process, a liquid solution containing a polymer is charged within an electric field with a reasonably high voltage (typically between 2 and 30 kV) that is sufficient to draw the liquid into fine sub-micron fibres<sup>113, 114</sup>. The fibres' diameter, morphology and length may be varied by changing parameters such as the solution viscosity, the molecular weight of the

dissolved polymer and the voltage difference between extrusion system and the reception support<sup>112-114</sup>. The incorporation of metal NPs into a polymer/solvent mixture was also performed<sup>129</sup> and after subsequent carbonization/annealing, led to the formation of metal/carbon rich nano-fibres<sup>130</sup>. However, issues related to the stability and interconnectivity of the metal NPs were raised and metal salt solution electro-spinning was shown to lead to the spinning of fibres with more controlled morphology and properties, Figure 5.

Although being an emerging technology, electro-spinning has a great potential for the preparation of sub-micron porous metal meso-structures. The versatility of the process may also lead to the preparation of metal alloyed fibres while the possibility to mixing a range of nano-fibres made of different metals or metal oxides may be particularly interesting for storage or bio-compatible materials, where only minute amounts of noble metals are required. The fabrication of porous metal frameworks from these nano-fibres may also find applications in filtration and separation where some metals' catalytic properties of the nano-textured surfaces and natural anti-microbial properties may be required.

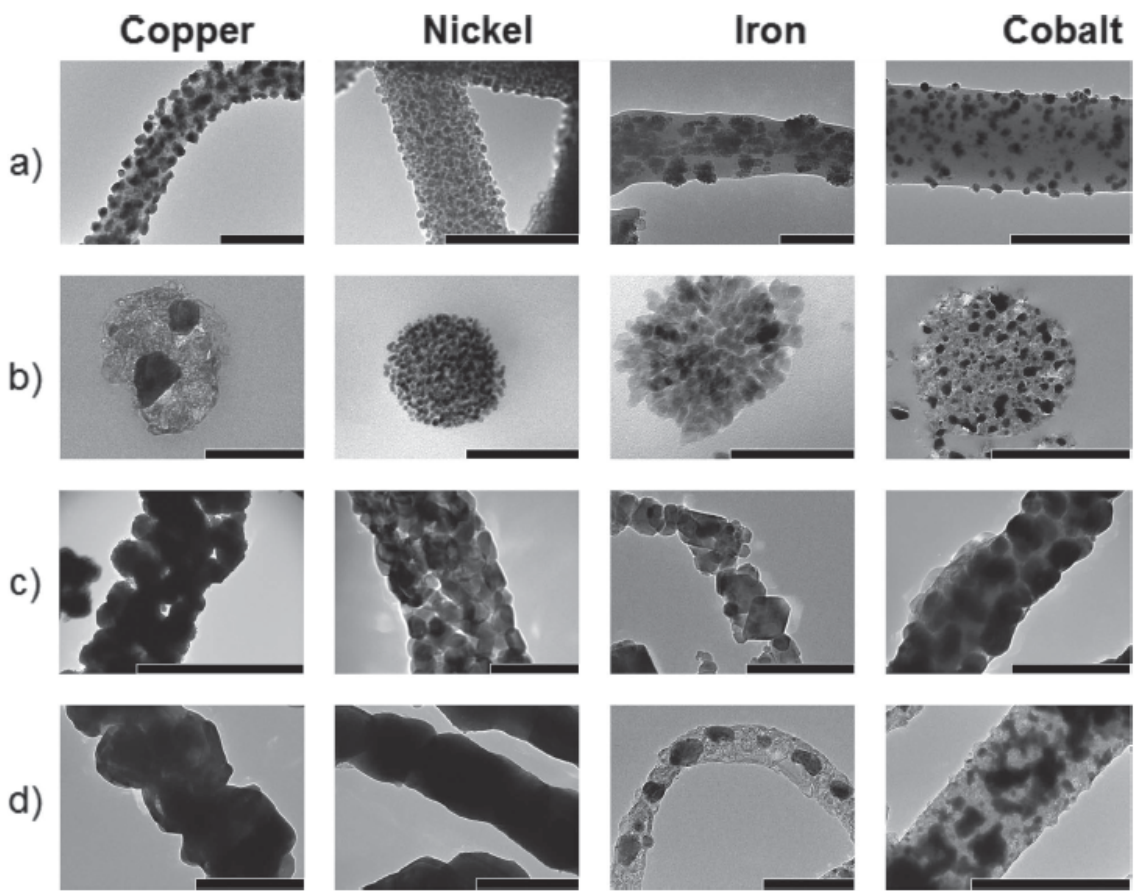


**Figure 5** Transmission Electron Micrographs of electro-spun metal nano-fibres, from <sup>126</sup>. The annealing conditions (a, b, c and d) were shown to be critical to form pure metal oxide materials and to remove most of the carbon deposited during carbonization

#### 2.4.4 Wet casting / drying or coating

Wet casting and drying involve the deposition of metal rich slurries onto appropriate supports, and can be used to produce thin films made of pre-dispersed metal NPs or hybrid metal-filler composite structures. The cast samples may generally require annealing or carbonization in order to remove the filler phase and produce a purely metallic porous material. Although dense metal supports have been extensively used for the preparation of H<sub>2</sub> permeable membranes, recent works have also demonstrated the potential of porous metal membranes for H<sub>2</sub> generation, exhibiting uniform pores of ~33 nm for a porosity of ~30%<sup>99, 131</sup>. This structure enhances the catalytic properties of the metal and favour H<sub>2</sub> generation and

diffusion, prior to separation from other gaseous or liquid species. Stainless steel (SS) hollow-fibres were processed by casting-drying slurries of SS macro-particles mixed with stabilizing agents and surfactants<sup>29</sup>. High fibre interconnectivity was obtained by post-casting sintering the entangled fibres at high temperature. An optimal sintering temperature of 1150°C was found to lead to an enhanced mechanical strength while maintaining sufficient porosity for high N<sub>2</sub> permeation. The pores across these structures were found to be relatively large (400 to 500 nm at 1150°C) due to the high fibre packing density.

This technique, that is easy to implement for the preparation of self-assembled metal layers, has not been demonstrated to form nano-porous structures. As for most metal NP assembly techniques, this is likely due to the difficulty of controlling thermal sintering<sup>64, 132</sup>. Although yet to be investigated, wet casting has great potential as an alternative technique for the preparation of large pore size macro-porous supports by electrical sintering<sup>63, 64</sup>. In this regard, electrical sintering was recently shown to be a smooth and slower-kinetics technique for the production of low density metal NP networks through charge transfer coalescence. Wet casting is particularly suited to electrical sintering if the casting support is judiciously chosen as an electrode. Although very much experimental, this technique could lead to a great enhancement in controlled metal NP coalescence and sintering - and this is an area of active research<sup>28, 133, 134</sup>.

## 2.5 Self-assembly of nano-particles

### *2.5.1 Block co-polymer metal conjugated self-assembly*

Ultra-thin and highly porous metal films have been synthesized with metal NPs using functionalized block copolymer self-assembly. A mixture of block co-polymer (BCP) and stabilized NPs<sup>36, 37, 135, 136</sup> have been spin coated onto a porous support to produce the filtration layer, Figure 6.

These films may be synthesized by using BCPs as templates and incorporating metal NPs into a given phase to create a BCP/metal NP hybrid. The morphology of the crystalline phases may be altered by varying processing parameters such as the BCP concentration or average molecular weight, the ratio of

the different monomers composing of the BCP, pH, temperature or additives<sup>137</sup>. Highly crystalline and ordered meso-structures may be obtained, allowing for fine control of the NPs distribution. Self-assembly occurs across multi-phase disorganized materials through a spontaneous process, typically involving either amphiphilic or a mixture of hydrophilic and hydrophobic molecules or molecular blocks<sup>136, 138</sup>. The thermodynamic incompatibility, typically seen as hydrophobic/hydrophilic interactions, between the n molecular blocks of the polymer, leads to micelle formation. The size distribution and morphologies of these micelles are therefore directly dependent on the properties, morphology and composition of the BCPs<sup>137</sup>. However, at thermodynamic equilibrium, macro-phase separation across the polymeric blend is prevented by the strong entropic interactions between the micelles and the solvent/BCP system. Therefore, in solution, the molecular blocks will be dispersed and form micelles above their critical concentration (CMC) and critical micelle temperature (CMT)<sup>139</sup> leading to a semi-ordered material made of two or more phases.

Although a number of crystalline phases can be obtained, both lamellar and hexagonal structures are typically sought after due to their high anisotropy. For instance, in the case of poly(ethylene oxide) (PEO)/poly(propylene oxide) (PPO) copolymers, it was shown that an overall BCP concentration of 60 to 70 wt% was necessary to obtain a hexagonal structure<sup>140</sup>. Variation of concentration or addition of NPs or nano-materials<sup>141, 142</sup>, such as carbon nanotubes<sup>140</sup>, leads to a change in crystalline structure, typically resulting in spherical shapes at low concentrations and lamellar structures at high concentration, while increased temperature was shown to re-organize micelles from spherical to rod-like structure<sup>143</sup>.

The incorporation of metal NPs may be performed either through direct mixing of metal NPs with a single BCP or a mixture of BCPs<sup>38</sup>, or by the *in situ* growth of metal NPs within the BCP macro-structure from metal precursors<sup>136</sup>. The addition of NPs into BCP was previously shown to affect the crystalline structure of the BCP by nucleating self-assembly<sup>140</sup>. A subsequent reducing step is generally used to stabilize the metal precursors into pure metal or metal oxide NPs. Higher metal loading can, however, be obtained through the mixing approach, as ligand-stabilized NPs can easily coalesce through thermal or electrical sintering into porous networks. The metal meso-structure can then be revealed through either evaporation or

carbonization of the solvent/BCP mixture<sup>144</sup>. In order to achieve high NP loading across the BCP matrix, the NPs should therefore: be easily suspended and dispersed in the solvent phase; exhibit preferential interaction with only one block of the BCP; and be smaller than the gyration radius of the preferred block. The BCP used should also be short enough to ensure a reasonable core/corona volume ratio to form at least two meso-structured phases<sup>136</sup>.

The main limitations of the formation of metal reinforced BCP self-assembled membranes reside in the control of the long range order of the crystalline structure. In addition, NP loading was found to be the limiting factor of the self-assembly process and high NP loadings led to highly organized and iso-porous hexagonal structures<sup>145</sup>. The size of the NPs is also suggested to dominate the pore size of the final porous structures, with larger NP size leading to larger pores. Metal NPs were either directly integrated into BCPs<sup>36, 135, 145</sup> or *in situ* synthesized by metal ion reduction<sup>146</sup>. Most work carried out to date on large scale BCP self-assembly requires the use of expensive BCPs, prohibiting their expansion for mass production<sup>145</sup>. Although promising, this technique is yet to be demonstrated on a larger scale and with less expensive BCPs. Further research is needed in this area, including a stronger theoretical understanding of both the interactions between surfactant molecules and NPs and the sintering mechanisms between nano-scale metal particles.

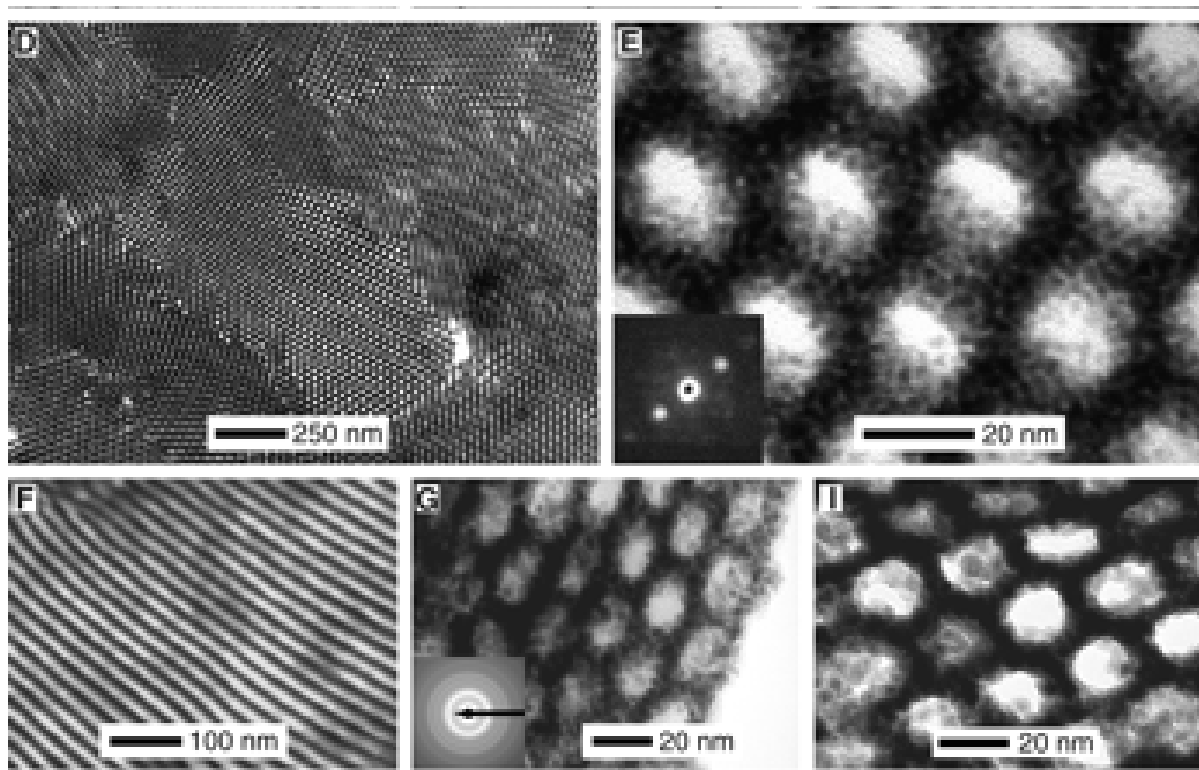


**Figure 6** Hexagonal phase formation by block copolymer self-assembly with 1-2 nm diameter metal NPs<sup>145</sup>. The different crystalline phases are visible in (d) while the high order of the gold NPs within the hydrophilic phase of the BCP is visible in (e, f, g and h).

### 2.5.2 Layer-by-layer assembly

Layer-by-layer (LbL) deposition of metal NPs on polymeric surfaces was also demonstrated to be an efficient way to form thin metal NP network films<sup>147</sup>. Decoration of porous metal structures with more catalytic NPs was shown to be a promising route to induce chemical degradation of contaminants, gas sensing or to enhance the electrical conductivity<sup>148, 149</sup> or magnetic properties<sup>150</sup> of non-conductive membranes or bio-materials. While LbL was performed within the pores and on the surface of polymeric hollow fibre membranes, it was also successfully used to decorate electro-spun nano-fibres<sup>151</sup>. The weak ionic interactions generated by the adsorption of poly-cations onto the surface of ceramic or polymeric materials represent a versatile way to functionalize non-conductive material surfaces with metal NPs. However, the stability of the deposited thin films is highly dependent on the solution pH and on the type of solubilized ions<sup>151, 152</sup>. The polyethylene imine

primer used in this work is stable at pH 8.5 and higher. A very low gold NPs adsorption was shown to occur at lower pH. In addition, to the best of the authors' knowledge, despite having been successfully used to catalytically reduce nitro-aromatic compounds, these surface coatings have not been used on model water based solutions containing more complex contaminants or exhibiting high salt concentrations. As shown in Figure 7, porous metal oxide structures can be readily processed through LbL, opening the route to form fine porous nano-structures on adequate nano-templates<sup>153</sup>.

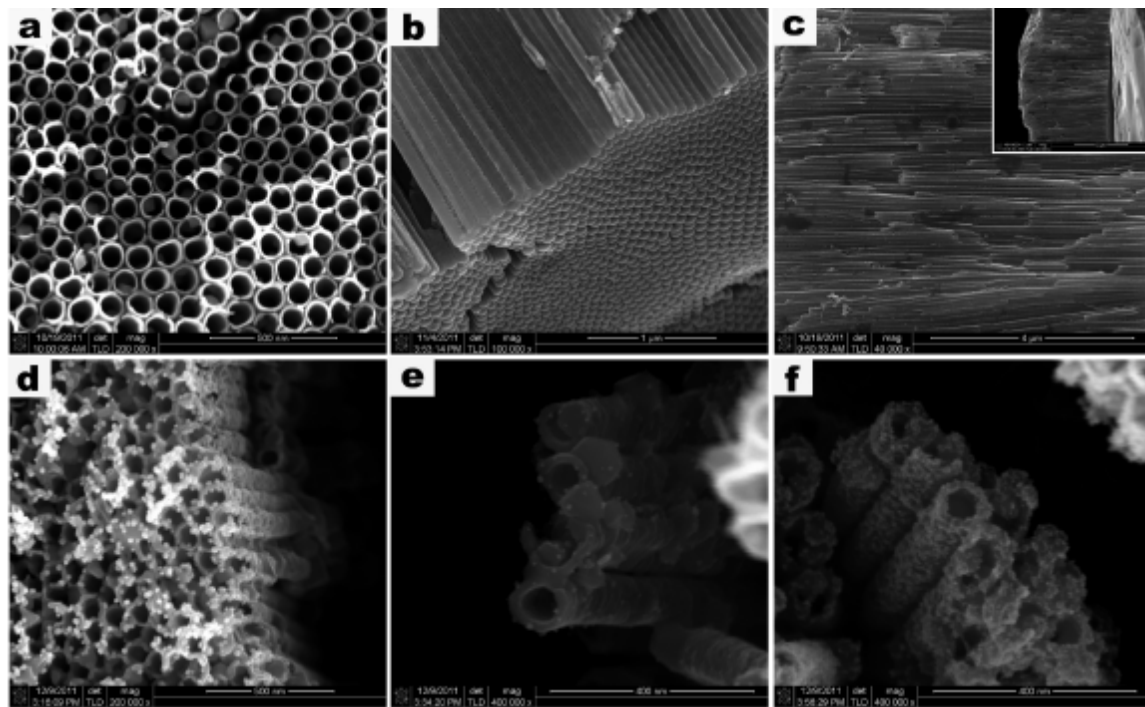


**Figure 7** LBL assemblies of titanium oxide nanotubes from <sup>153</sup>The alumina support (a, b) was used to deposit titania at different rates (c, d) leading to well-built titania CNTs after template removal.

### 2.5.3 Ink-jet printing

Ink jet printing may be used to precisely fabricate intricate layers on either flat or 3D substrates by depositing thin films of particles that were mixed into a gel solution with either a polymeric or an inorganic ligand<sup>154</sup>. A micron thick layer of this

gel is then deposited at high shear flow onto the printing substrate. This high-throughput technique, that is able to prepare patterned structures down to the micron resolution<sup>155</sup>, is also highly promising for the preparation of thin film porous metal structures. The large range of printing substrates makes ink-jet printing one of the most versatile techniques to date for the synthesis of multi-layer composite materials<sup>156, 157</sup>.

Room temperature sintering via ink jet printing was demonstrated to occur for metal nano-particles<sup>73</sup>. Sintering of closely packed silver NPs via this route was demonstrated to lead to a semi-dense network with porosity and pore size ranging between 10 and 40 % respectively (as evaluated from Scanning Electron Micrograph analysis - Figure 8), and 40 to 150 nm respectively at room temperature without pressure<sup>73</sup>. As per other self-assembled metal NPs routes, coalescence of NPs has been shown to occur naturally at room temperature in NP agglomerates in order to minimize surface energy, by increasing the specific surface area<sup>158</sup>.

The scope of application of metal particle ink-jet printing is relatively large and ranges from the preparation of bio-compatible or lithography mask surfaces to the preparation of micro-fluidics or electro-mechanical devices<sup>92, 154, 159, 160</sup>. It might be possible to prepare more refined structures with pore size distributions below this 40 nm benchmark by better controlling the deposition mechanisms and post-treatment conditions. The adequate use of smaller metal NPs could lead to the preparation of narrower pore size and larger porosity materials<sup>132</sup>. The stabilization of the NP network and the control of the mechanical properties of the layers are, however, once again critical issues to be studied and solved in order to allow for an extension of this technique to the mass production of thin porous metal films.

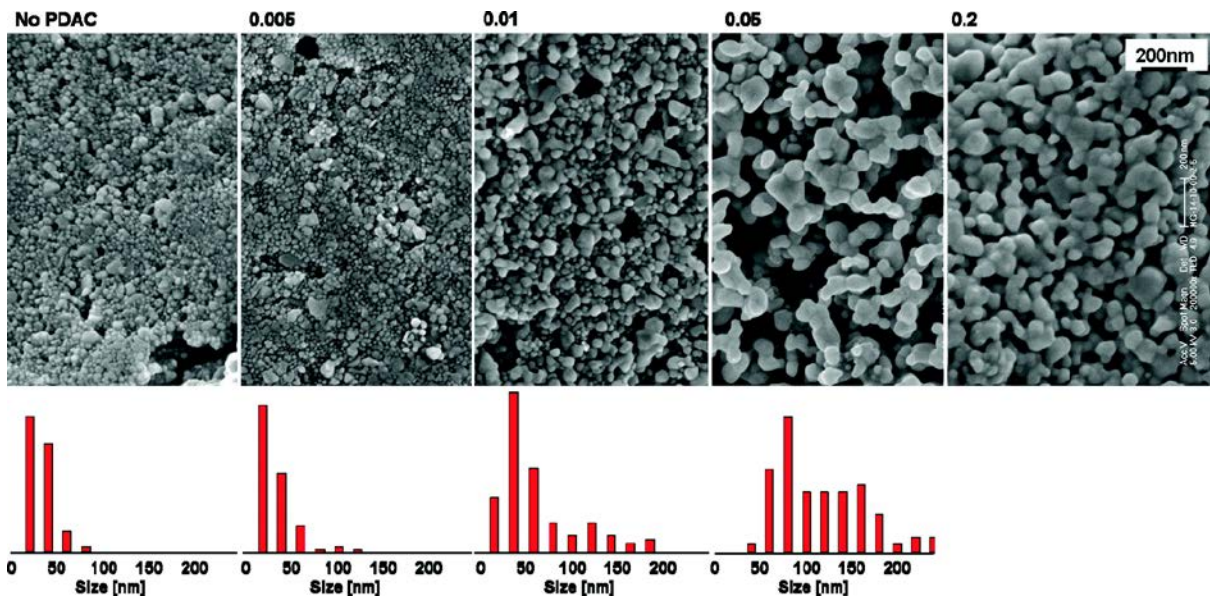


**Figure 8** Room temperature sintering used in ink-jet printing process <sup>73</sup>. The progressive addition of Poly (diallyl-dimethyl ammonium chloride) (PDAC) led to an increase of the average particle size and stabilized the network to form sub-100 nm pores between the particle aggregates.

## 2.6 Thin film de-alloying

Chemical or electro-chemical oxidation of noble metal surfaces was demonstrated to be an efficient way to create or widen pores across metal thin films and has the potential to lead to the preparation of porous metal frameworks. It is essentially a selective etching process whereby a number of metal phases are removed from an alloy matrix. The noblest phase will remain, forming the pore walls of the future metal porous framework. A variety of either oxidative or reductive chemical etching solutions such as sulphuric acid <sup>161</sup>, hydrochloric acid<sup>162</sup> or sodium hydroxide<sup>163</sup> have been used to selectively etch away metals. Electro-de-alloying has also been carried out and typically leads to finer structures due to the greater metal etching selectivity. De-alloying has been used to prepare catalysts<sup>164</sup>, electrodes, actuators<sup>165</sup> and diffusion membranes<sup>166</sup>.

De-alloying of multi metal alloy films was shown as a way to create nano porosity across pre-deposited metal structures<sup>167</sup>. Both pore size and morphology are strongly related to the material grain size and to the relative metal content within

the alloy. Narrow pore size distribution can be achieved across metal thin films if the metal mixing is good and if one of the metals can be selectively removed over the other without affecting the grain network. Templating / de-alloying was recently performed in order to fabricate hollow nano porous gold shell assemblies<sup>168</sup>. The initial Ag/Au coating was obtained by electroless deposition of metals onto poly(styrene) (PS) nano-spheres. After carbonization of the polymer template, Ag metal was removed through a diluted nitric acid treatment which produced porous monoliths exhibiting pore sizes ranging between 20 and 30 nm and porosity close to 50%, corresponding to the initial Ag content within the alloy<sup>90</sup>. Furthermore, fine nickel oxide films were recently converted into full nickel metal porous structures by annealing and reduction of the metal oxides at 400°C. The porous metal oxides exhibited porosity close to 50% and pore size distributions between 100 and 500 nm<sup>26</sup>, Figure 9. The use of highly noble metals unaffected by chemical or electrochemical etching, within pre-formed metal alloy films, containing gold for instance, can lead to very well organized structures with narrow pore size distributions, as seen in Figure 10. In addition, the fabrication of de-alloyed multi-layer metal sheets by selective etching of copper exhibited a gradient of porosity and pore size across silver/copper films<sup>169</sup>. The dual-layer structure was due to a strong atomic ratio gradient of silver over copper across the thin films, which led to a pore size between 182 and 264 nm. The interface between the two layers was found to be atomically smooth and homogeneous, which opens the route to the fabrication of asymmetric porous metal structures.

De-alloying is also a fast sample processing route that can selectively etch metal oxides or metals from multi-phase alloys. The major strength of the de-alloying technique therefore lies in its high production throughput and ability to prepare nano-scale pores within the range of ~ 20 to a few hundreds of nano-meters. The control of the metal alloy texture and grain size is critical and very fine grain textures are required in order to further reduce the pore size of final de-alloyed thin films below the 20 nm benchmark. Although hardly studied to date, the potential of multi-phase or gradient-phase de-alloying is also very important and could lead to very homogeneous structures with tuned pore tortuosity and pore shape - with potential applications in separation science.

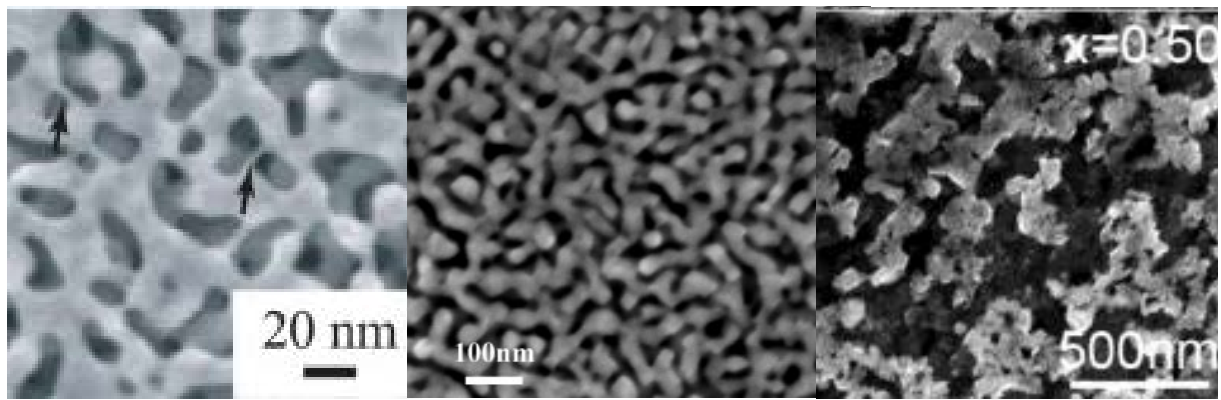


**Figure 9** Scanning electron micrographs of different de-alloyed structures from (left) de-alloyed Ag/Au (50/50) leaves <sup>11</sup>; (centre): Cu/Mg (30/70) <sup>170</sup> and (right) Cu/Ni (50/50) <sup>171</sup>.

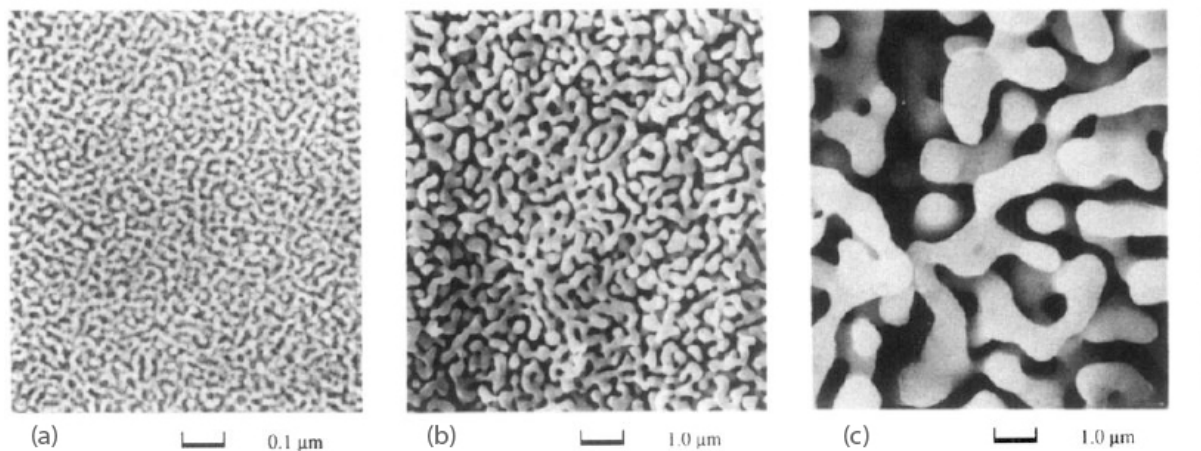


**Figure 10** Scanning electron micrographs showing the interpenetrating solid-void composite structure of the porous Au. The de-alloyed samples were annealed at the indicated temperature for 10min. (a) 100 °C, (b) 500°C and (c) 700°C <sup>172</sup>.

## 2.7 General morphology of porous metal frameworks

The relation between material morphology and the main techniques presented in this review are presented in Table 1. The morphology of porous nano-structures depends directly on the processing technique. As discussed in the previous section, a number of parameters are critical to form porous metal frameworks with adequate pore shape, size and morphology. The most critical parameters to be controlled and

investigated include pore interconnectivity, pore size distribution and overall porosity in order to either ensure high permeation across the material or to provide high specific surface contact area.

Although, to date, sintering and foaming are the most mature technologies for the preparation of commercial porous metal frameworks, these techniques do not allow great versatility in terms of membrane morphology and nano-scale pore size control. Most of the sintered commercial membranes exhibit porosity below 40% and pore sizes larger than 500 - 600 nm. The macro-properties of porous metal frameworks, such as their thermal, mechanical or electrical properties, are directly related to the interconnectivity and stability of the network. This has been especially documented for sintered materials and more research effort should be dedicated towards a finer control of their porosity, tortuosity, and pore size distribution<sup>173-175</sup>. The prohibitive costs associated with raw metal materials should also be taken into account when competing with cheaper commercially available polymeric or ceramic materials. Alternative routes to prepare porous metal frameworks, requiring less energy, generating less waste materials, or allowing greater material recovery and recycling should also be considered.

Although metal NPs fabrication and assembly, as beads or fibres, either by self-assembly or ink-jet printing, are attractive due to their enhanced surface properties, such as specific surface area and high morphological versatility, issues with the stability of the metal NPs and interfaces during sintering are limiting their current development. Further research is needed to improve the understanding of metal NP coalescence mechanisms and to find routes to stabilize the particles into well-ordered or interconnected networks in order to fabricate reproducible meso-structures. Ink-jet printing appears to be the most suitable technique for the preparation of thin film porous NP assemblies as it allows for fast processing rates and can be applied to a variety of substrate shapes and morphologies. More work is needed to provide a sustainable fabrication route towards nano-scale pore formation. One of the most promising (emerging) porous metal fabrication routes appears to be selective de-alloying, as it is a fast, cheap and highly up-scalable technique. De-alloying of specifically designed metal alloys, such as those comprising an atomic gradient content or made of layers with multiple grain size distributions, have great potential in the fabrication of asymmetric materials. The preparation of such

materials, likely by electroless deposition or electro-deposition, can open the route to the fabrication of highly controlled pore morphology and tortuosity, which is fundamental to the customized development of porous metal frameworks for specific applications. Recent developments in the fabrication of large arrays from stable metal nano-particles<sup>176-178</sup> and in the functionalization<sup>32</sup> or coating of metal surfaces<sup>179</sup>, may further push the envelope of the these techniques leading towards the fabrication of nano porous materials with a pore size below the 20 nm benchmark. In addition, the synthesis of multi-metal alloy films or NPs<sup>180</sup> could also lead the way to the processing of nano-textured alloys, with multiple nano-porosities, for use in de-alloying processing routes.

Another important route which warrants further enquiry, concerns the combination of different fabrication techniques. For instance, the development of weak foam structures could be mechanically reinforced by electro-deposition or electroless deposition of metals at the thin necks between the metal cells. The synergies between different strategies might lead to a much better final outcome, limiting the drawbacks of some of the techniques requiring post-sintering, for example.

Table 1 Summary of the different fabrication techniques with indicative minimum pore size achieved, ranges of porosities and overall morphologies and advantages and drawbacks

Techniques	Pore size	Porosity (%)	Morphology	Advantages	Drawbacks
<i>Direct casting</i>	5 to 500 µm <sup>+</sup>	40 - 60	Straight pores or random network	Highly up-scalable and cheap Large range of sacrificial phases	Large pore size and need for carbonization
<i>Foaming</i>	>50 nm	50 - 95	Highly random network, open or closed cells	High through-put, cheap and mechanically resistant Large versatility in shape forming Mature technology	Large pore size distribution and difficulty to reach nano-scale pore size; presence of closed cells Mechanical stability might be low
<i>Thermal sintering</i>	>300 nm <sup>+</sup>	30 – 60 <sup>+</sup>	Random network of assembled particles High tortuosity	Easily up-scalable Mature technology Cheap to process	Coalescence of particles, issues with stability, thermal energy is expensive
<i>Electrical sintering</i>	>30 nm		Random network of assembled particles High tortuosity	Finer structure than thermal sintering as energy is better transmitted	Very thin films only reported to date due to electrical current diffusion (< 250 nm)
<i>Electro-spinning</i>	>50 nm	50 - 75	Straight or random pore network between fibres	High up-scalability, great versatility and relatively cheap	Weak mechanical strength, need for post-treatment including sintering and carbonization
<i>Self-assembly</i>	>10 nm <sup>+</sup>	40 – 60 <sup>+</sup>	Porous entangled network to highly ordered pores (opal shape)	Great versatility depending on template and particle shape and size Easy to combine different metals	Slow and difficult to control over large scales Limitation due to necessary post-treatments including sintering
<i>Ink-jet printing</i>	>50 nm	40 - 60	Straight pores with low tortuosity to highly entangled	Extremely high through-put Versatile to cover 3D surfaces	Need for post-treatments such as sintering or carbonization

			network depending on size of the particles and processing conditions	Able to control thickness and printing dope composition towards multiple layers or different metals composition Great potential for lithography deposition	Promising but still immature
<i>Electroplating</i>	>1 µm	40 - 60	Straight pores with low tortuosity to highly entangled network depending on the substrate	Potential as a binding technology onto pre-formed porous metal networks (of large pore size)	Requires a conductive substrate or pre-treatment onto the surface to be plated  Large grain size distribution leading to large pores or low porosity
<i>Electroless deposition</i>	>10 nm <sup>+</sup>	30 - 70	Straight pores with low tortuosity to highly entangled network depending on the substrate	Very fine grain size formation  Able to replicate virtually any substrate shape and morphology  Excellent at depositing ultra-thin layers and processing nano-scale pore size distribution	Very slow kinetics of diffusion  Requires great control of the plating bath composition, pH, temperature  Sensitizing agents are critical to selective deposition
<i>De-alloying</i>	>20 nm	10 - 90	Random network of pores depending on the grain size, homogeneity of the alloy and de-alloying conditions	Very versatile, cheap and high-through-put technique  Symmetric, homogeneous or heterogeneous and asymmetric materials	Mature technology that has not been highly applied yet due to the difficulty to prepare ultra-thin layers of fine grain size alloys

\* Insufficient data to estimate a range

+ Variable depending on the substrate, template or sacrificial phase morphology

### **3. Chemistry of metal surfaces**

Functionalization of metal surfaces can be beneficial to the dispersion and stabilization of metal NPs in solution<sup>181-184</sup>. Conjugation with organic molecules such as ligands<sup>185, 186</sup> or proteins<sup>12, 187, 188</sup> may enable NP self-organization<sup>189, 190</sup>, or may protect against corrosion<sup>191, 192</sup>. In regard to the latter, metal surfaces are naturally prone to oxidation under most industrial and day-to-day applications leading to a generally high level of metal oxidation on their surfaces. This section presents the major routes that have been demonstrated to lead to strong covalent bonding to both metal oxide and pure metal surfaces that can be used to fine tune the materials' properties. Although very few of these routes and chemistries have been applied in metal frameworks science to date, the nature of the interactions in solution between the membrane surface and both solvent and potential contaminants makes surface functionalization an inevitable step in the further development of porous metal membranes. A strong focus on NP functionalization has been given to this section since this is expected to be associated with enhanced reactivity. This section does not attempt to be comprehensive but rather to provide a guide to the reader of the most commonly used chemistries.

#### 3.1 Chemistry on metal oxide surfaces

General interest in metal oxide NPs is increasing because of their interesting optical and magnetic properties<sup>182, 193-195</sup>. A number of modifiers, including thiols, carboxylic acids or amines<sup>196-198</sup> have been successfully grafted onto metal oxide surfaces. The most popular routes to modifying metal oxide nanoparticles are through the addition of phosphonate or silane ligands, since the functionalization routes are better understood. Although ligand exchange on a metal oxide NP surface is possible these reactions are generally not favourable, since both incoming and outgoing ligands must exhibit similar charge and be able to fit into the exact same number of coordination sites<sup>199</sup>. Metal oxide surfaces must, therefore, rearrange to accommodate the addition of extra ligands within the limits of steric hindrance and thermodynamically viability.

### *3.1.1 Carboxylates*

Carboxylate ligands, such as fatty acids, are often used for modifying metal oxide NPs<sup>200</sup>. For example, the binding of carboxylate ligands onto the surface of titania nanoparticles with various controlled sizes from 0.7 to 6.0 nm has been investigated and it was shown that the surface binding energies are NP size-dependent. The overall chemisorption of carboxylate groups increased with a decrease in NP size - leading to denser surface coverage<sup>201</sup>. Carboxylate coupling was also reported on various metal oxide surfaces such as silicon<sup>202</sup>, copper<sup>203</sup>, iron<sup>203</sup> and tungsten oxide NPs<sup>203</sup>.

### *3.1.2 Silanes*

Silanes are the most popular surface functional groups grafted onto metal oxide surfaces. This is mostly related to the very broad choice of commercial silanes available, and to their relative facile synthesis on laboratory scale. Furthermore, silanes can also be introduced simultaneously with the metal oxide precursors through simple and high yield sol-gel reactions<sup>204</sup>. Silanes are also able to support numerous functionalities on their backbone chain, such as amino, cyano, carboxylic acid or epoxy groups<sup>32, 205-209</sup>, making them very versatile compounds either for direct functionalization or for use in intermediary steps. Silanes have been grafted onto numerous metal oxides such as SiO<sub>2</sub>, Al<sub>2</sub>O<sub>3</sub>, TiO<sub>2</sub>, SnO<sub>2</sub>, ZrO<sub>2</sub>, and V<sub>2</sub>O<sub>5</sub>. A disadvantage of silane sol-gel condensation residues is the production of reaction by-products that can alter the metal oxide NPs. Magnetic ferrite NPs were shown to dissolve readily upon reaction with chloro-silane because of the liberation of HCl<sup>210</sup> as a reaction product. If performed carefully, silane chemistry remains a highly competitive method that leads to dense surface coverage<sup>211, 212</sup>.

### *3.1.3 Phosphonate*

Analogous to silanes, surface grafting of phosphides occurs through the formation of a metal–oxygen–phosphorus bond. These reactions are generally thermodynamically favourable and able to occur over a large pH range, as with

titania<sup>213, 214</sup>. As opposed to silanes where unstable Ti–O–Si bonds are formed, Ti–O–P bonds are very stable with respect to hydrolysis, making them promising grafting agents for aqueous membrane applications. Phosphorus, like silicon, is able to expand its coordination number to form stable hyper-coordinated phosphorus species<sup>215</sup>. In addition, as opposed to silanes where Si–O–Si reactions can occur, phosphonates will not cause homo-condensations that has the advantage of increasing the grafting yield<sup>197</sup>. Alumina, tin oxide, zirconia and magnetite were also shown to be readily functionalized with phosphonate groups<sup>6, 214, 216-218</sup>. In addition, due to larger steric hindrance effects, phosphonate groups may also form multiple anchorages onto metal oxide surfaces, further stabilizing the structure<sup>219</sup>. Although phosphonate modification is a very powerful method for functionalizing metal oxide surfaces such as alumina or titania, the relatively unstable Si–O–P bonds formed are more sensitive to hydrolysis compared to most other metal–oxygen–phosphorus bonds<sup>215</sup>. For this reason, the use of phosphonate is mostly limited to non-siliceous particles<sup>214, 220</sup>.

### 3.2 Chemistry on pure metal surfaces

The types of chemical groups that can be readily grafted onto pure metal surfaces differ markedly from those applied to metal oxide surfaces. In the case of metal oxides, covalent bonds are generally formed via the oxygen atom(s) bridging the metal to the relevant functional group, while in the case of pure metals grafting is related to the direct metal coordination of the relevant functional group and therefore to sharing electrons between the unsaturated electronic band of a Lewis acid and excess electrons from a Lewis base. Therefore, general pathways for pure metal functionalization may lead to unstable bonds that can be impaired through the input of thermal, chemical or electrical energy<sup>221, 222</sup>. Pure metal nanoparticles have been successfully functionalized with thiols<sup>204, 223, 224</sup>, di-sulfides<sup>200</sup>, amines<sup>223, 225-227</sup>, nitriles, carboxylic acids and phosphines<sup>225, 226, 228</sup>. Selected examples will be presented in the following sections. Although mostly focused on noble metals, such as gold, silver or platinum, most of the chemisorption routes described in this section should also be applicable to less noble metal surfaces such as iron, copper, aluminium or nickel.

### *3.2.1 Thiols and Di-sulfides*

The grafting of organo-sulfuric groups to metal nanoparticles is amongst the most developed routes, since such groups strongly coordinate to various metals, such as Ag, Cu<sup>229</sup>, Pt, Hg, Fe, Li<sup>230</sup> or Au<sup>231</sup>. The metal-sulphur interaction is strong enough to immobilize the thiol groups on the surface of metal nanoparticles. The chemisorption energy between gold and sulfur was estimated at 126 kJ.mol<sup>-1</sup> and shown to require two gold atoms per thiol group<sup>232</sup>. The strength of interaction however strongly decreases upon oxidation of the thiol group to sulphate or sulphonate<sup>233</sup>. In addition, aromatic thiols were shown to occupy various coordination/adsorption sites on the metal surface with very small energy differences between them, suggesting additional electrostatic interaction between the aromatic ring and the surface which is highly dependent on the aromatic ring orientation relative to the gold surface<sup>233, 234</sup>. Thiols and di-sulphides can either readily physiorb on the metal surface or chemisorb through the splitting of the sulphur-hydrogen bond of the molecule, thus generating a negatively charged group<sup>235, 236</sup>. This was demonstrated spectroscopically for methyl-thiolate chemisorption onto gold surfaces where methyl-thiolate radicals covalently bind to gold without any metal-thiol charge transfer<sup>237</sup>.

Organic-sulfur compounds can also be capped onto metal surfaces through a two stage process. The first step is very rapid and depends on the concentration of the organo-sulfur compound in solution. During the second step, the organic groups bonded to the sulfur atoms interact with each other and reorganize themselves to minimize energy and enhance the stability of the adsorbed layer. The grafting kinetics of the second step is directly linked to ligand-ligand interactions<sup>200</sup>. It is, therefore, possible to substitute thiols present on the particle surface with different functionalized thiols through thiol-thiol substitution<sup>225, 238</sup>. This procedure is interesting for the functionalization of nanostructured surfaces where the organic function to be introduced is not compatible with the synthesis conditions of the pure metal surface<sup>239</sup>. The stability of thiols is limited and thiols were shown to desorb during aging in biological media<sup>224, 240</sup>, which was directly related to the electronic structure of the metal particle core<sup>228</sup>.

### *3.2.2 Amines and Ammonium Ions*

Amine functionalization of pure metal NPs was generally performed in order to stabilize particle suspensions<sup>225</sup>, as demonstrated for hexa-decylamine grafted Pd NPs<sup>226</sup>. A common method to stabilize noble metal NPs is by adsorption of tetra-alkyl-ammonium halides - as the long alkyl ammonium ion chains exhibit amphiphilic properties, allowing the creation of well dispersed micelles<sup>241</sup>. Hydrophobic metal NPs and surfaces, stabilized with long alkyl ammonium ion chains, can be rendered hydrophilic through this process<sup>227</sup>. Although interactions between amino groups and metal NP surfaces are much weaker than those of thiol terminated compounds, large proteins and peptides were shown to link to silver NPs through both thiol and amine functionalities<sup>223</sup>.

### *3.2.3 Carboxylic acids*

Deprotonation of carboxylic acids, into carboxylate groups, was also shown to lead to bridging with metal surfaces<sup>223, 242, 243</sup>. Although not strong chemisorption, Density Functional Theory (DFT) calculations performed on the attachment of N-isobutyryl-L-cysteine to gold NPs suggested that both thiol and carboxylate functions were involved in surface binding, while that of penicillamine involved the thiol, amine and carboxylate groups. The stability of such systems may be dramatically enhanced owing to the multiple attachments of each function group providing sufficient stability to maintain chemisorption<sup>223, 244, 245</sup>.

### *3.2.4 Phosphine*

The attachment of phosphine groups onto metal NP surfaces was shown to be easily achieved<sup>225</sup> but to led to very weak bond energies<sup>225, 228</sup> and subsequently to very poor stability of the NPs in solution. The lack of stability results in an easy exchange with other ligands, such as complete exchange with thiols, as thiols bind more strongly to the metal surface<sup>225</sup>. This exchange capability can be used in synthesis as an intermediary step towards more complex thiol attachment which

cannot be readily grafted due to steric hindrance. Tri-phenyl-phosphine was previously grafted onto gold NPs<sup>228</sup>. Although similar substitutions occur between amine and phosphine ligands, less stable gold particles were obtained<sup>225</sup>. The lack of stability of phosphine ligands can be partially overcome by introducing poly-phosphine ligands as previously demonstrated for bis (diphenylphosphino) - decane or bis (diphenyl phosphinoethyl) phenylphosphine functionalized palladium NPs<sup>226</sup>.

### 3.3 Summary

A number of surface functionalization routes have been demonstrated to produce stable surface coatings. The control of surface energy is a critical aspect of porous material design as processing high specific surface area materials is not sufficient to enhance the bulk materials properties. The formation or deposition of nano-textures through specific grafting of chemical groups, in order to favour specific chemical interactions with the surrounding media, or to control liquid wetting across the pores or to protect the metal surface, is crucial to the processing of advanced functional porous metal frameworks. Clear functional pathways have been developed to provide metal corrosion protection or to tune surface energy for specific adsorption or grafting, but more research is needed to test the impact of these structures and functionalities on the properties of final materials.

## **4. Major fields of application of porous metal frameworks**

### 4.1 Heat storage and dissipation

Open cell metal frameworks of high porosity have emerged as attractive heat exchange media for a wide range of applications where large surface to volume heat dissipation is required<sup>246, 247</sup>. These periodically structured materials composed of stacked metal meshes or foams, must present well-ordered morphologies with low porosity and large interconnected through pores in order to act as efficient heat sinks<sup>21, 248</sup>. In addition to their morphology, these materials must also offer high thermal conductivity and diffusivity<sup>16, 247, 249, 250</sup>. The thermal and fluid flow characteristics of such woven metal textiles were comparable to plate-fin heat exchangers while being up to 40 % lighter. The continuity of the metal phases and the structure of the micro-lattice<sup>250</sup> were also critical<sup>234, 251</sup> as sintered metal materials exhibited higher thermal conductivity than solely packed metal materials. Forced convective heat transfer in packed beds of sintered and non-sintered copper spheres, for instance, demonstrated that sintering significantly increases the overall heat transfer coefficient and heat dissipation rate due to the reduced thermal resistance of the material<sup>247, 252</sup>. The crystalline structure and composition of the nodes interconnecting the metal particles, ligament or fibres also greatly affect heat dissipation<sup>253</sup>. The forced air convective thermal efficiency of brazed metal fibre woven structures was, for instance, up to three times larger than that of open-celled metal foams, primarily due to a lower air flow resistance during coolant circulation through the porous metal framework pores<sup>252</sup>.

The development of asymmetric porous metal frameworks may therefore lead to better heat flow control across the material and act as specific heat channels, towards co-regeneration or energy transfers. Similarly, the development of novel alloys and a better understanding of the sintering mechanisms at the nano-scale may also greatly improve heat transfer dynamics towards more efficient and cheaper heat dissipation materials. Ageing of these materials may also be an issue that has not been substantially investigated to date as porous metal materials exhibit enhanced surface to volume ratio and are subsequently more prone to oxidation and degradation. Changes in thermo-mechanical properties over time and under such

drastic heat transfer conditions may therefore affect the long term stability of the materials.

#### 4.2 Reinforcement for composite materials

Porous metal frameworks have been incorporated with ceramics and polymers to form dense hybrid composite materials with highly versatile and tuneable properties<sup>254</sup>. Combining the properties of porous metal structures along with other functional materials has been demonstrated across fields such as the automotive, building and aerospace industries, printing, and acoustics<sup>255, 256</sup>. The nature of the interface between the different phases will here play a great role in the overall thermal, electrical or mechanical properties of the composite materials<sup>257</sup>. The characterization of the pore interconnectivity, surface roughness, adhesion or binding of the different materials has therefore been one of the primary focuses of their development<sup>258-261</sup>. The fabrication of lightweight materials with enhanced thermo-mechanical properties is of interest to reduce operating costs and energy requirements in the automotive and aerospace industry<sup>262, 263</sup>.

Controlling the interface and the affinity between the reinforcing metal and the filling matrix continues to be the main challenge with the incorporation of such porous metal materials. . Metal materials of high surface area are more reactive to oxidation and degradation mechanisms and must therefore be protected, either through the introduction of gas impermeable materials or by controlling the thickness and composition of the oxide layer on their surface.

#### 4.3 Sensors, actuators and electrodes

Porous nano-structured metal electrodes, exhibiting typical surface areas a few decades larger than similarly dimensioned planar electrodes, and consisting of either anisotropic or random pore distributions have received considerable attention in recent years<sup>264</sup>. These electrodes are of particular interest for chemical, water vapour or gas sensing<sup>265, 266</sup>, as lower detection limits can be achieved<sup>10, 11, 193, 264</sup> and for electro-analytical chemistry, where rates of reactions are interface

dependant<sup>267, 268</sup>. Porous metal actuators have also been produced by metal foaming<sup>269</sup>. The increased surface of exchange can lead to larger Faradaic currents<sup>267</sup> and to higher signal to noise ratios, enhancing the sensitivity of the sensor response electrode. Noble metal electrodes of high surface area have been fabricated using a number of different approaches including hard templating of poly(styrene) spheres or silica spheres<sup>28, 270, 271</sup>, chemical de-alloying<sup>11</sup>, electrochemical de-alloying<sup>39</sup>, electroless deposition within the pores of nano-porous membranes as well as from sintered metal NPs<sup>232, 270</sup>, and electro-spun metal webs<sup>272, 273</sup>.

To date chemical de-alloying and electroless deposition appear to be the most mature technologies for the preparation of metal based nanoscale porous sensors and electrodes. The natural electrical and thermal properties of metal structures are obviously great advantages in this field compared to ceramic and polymeric materials but greater work is needed towards the development of nano-porous materials for specific detection, channelling or separation. The large range of chemical groups that can be grafted onto metal surfaces make porous metal frameworks highly promising candidates for integration into advanced electro-active materials.

#### 4.4 Orthopaedic and biomedical use

A large number of porous metal frameworks have been developed as mechanically strong bio-compatible materials for a range of medical and orthopaedic applications. Traditional metallic bone implants based on light and soft metals such as nickel, stainless steel or aluminium<sup>9, 274, 275</sup> are typically dense and are prone to oxidation-reduction reactions as well as exhibiting a lack of adequate space for biological tissue growth<sup>276</sup>. New architectures based on mimicking the morphology and properties of natural bone have been developed based on macro-porous metal structures. The use of biocompatible and corrosion resistant metallic materials to reduce or prevent adverse anti-body reaction and graft rejection have been successfully demonstrated primarily through the use of titanium and some of its alloys. These materials offer excellent biocompatibility, high strength-to-weight ratio, a lower elastic modulus compared to traditional materials, and superior corrosion resistance<sup>274</sup>. Powder metallurgy and space holder sintering are the two main routes

for the preparation of these micron-pore size metal frameworks<sup>275</sup>. Pore shape, porosity, and pore size distribution, were adjusted across hundreds of microns as desired for osteo-conductive applications<sup>277, 278</sup>. Porous bio-compatible metal frameworks offer high elasticity and mechanical ageing resistance which are necessary for most load-bearing applications in fracture fixation and bone replacement<sup>276, 279</sup>.

Although relatively limited in terms of research, the development of functional groups on the surface of the porous metal materials may further improve biocompatibility and the interface with biological cells.

#### 4.5 Membrane separation

Metal micro-filtration (MF) membranes have been used in a number of studies related to liquid and slurry food preparation and filtration, including dairy, fruit juice and alcohol<sup>280</sup>. Metal membranes were here shown to be competitive against polymeric membranes as facile cleaning can be performed by high pressure back-flushing of the modules, limiting the need for and impact of cleaning chemicals. The stability of metal membranes during steam sterilization is also an advantage in food processing where high frequency cleaning and disinfection of the membrane materials are desired to prevent bacterial contamination. Notably, porous metal membranes have especially been used in a number of water applications including MF, membrane reactors and bio-reactors, electrolyzers and membrane evaporators<sup>151, 281-288</sup>. The catalytic properties of pure metal and metal decorated membranes have been particularly sought after for in water treatment (Table 2). Denitrification, corresponding to the conversion of nitrates into nitride, was demonstrated to be enhanced with alumina coated palladium and copper NPs<sup>44, 287, 289</sup>. Smaller grain size led to higher activity coefficients<sup>287</sup>. Micro-filtration ozone assisted experiments were also demonstrated to limit surface fouling on metal membranes by activating the metal surface. This led to a decrease of the cleaning frequency and was shown to be beneficial when metal membranes were used as pre-treatment steps in dual systems with electro-dialysis<sup>290</sup>. Desalination was also demonstrated with porous metal membranes by membrane evaporation, a novel desalination technique using metal membranes both as heating elements and porous separation layers between a saline feed and an air-gap. The principle behind

metal evaporators is close to that of air gap membrane distillation except that the feed-water is not heated by the membrane<sup>291-294</sup>. This technique is highly promising but requires hydrophobic porous membranes to efficiently desalinate water. In this regard, stainless steel membranes have been coated with hydrophobic poly(dimethyl-siloxane) (PDMS) and heated through exposure to ultra-violet lamp<sup>291-294</sup>.

A number of challenges remain and should be tackled to offer more specific solutions to unsolved engineering and separation problems. While metal membranes offer clear advantages over polymeric membranes in seawater pre-treatment and abrasive liquid purification, current commercial metal membranes have limited scope for applications due to their inadequate pore size and shape that is inherent in their fabrication process. To date, commercial metal membranes are either processed by sintering<sup>62, 295</sup> or foaming<sup>18</sup>. These fabrication processes typically lead to large pore size ( $> 1 \mu\text{m}$ ), low pore connectivity and limited porosity (<50%)<sup>62</sup>, and do not offer separation properties sufficient for fine particle separation such as those achieved by polymer membrane ultrafiltration (pore size 10 to 100 nm). The optimization of surface properties of these commercial metal structures has not been systematically investigated despite the demonstrated potential for metal surfaces to exhibit strong catalytic activities due to their partially unsaturated electronic state facilitating chemical oxidations<sup>96, 296</sup>. Therefore, the opportunity exists to develop new processing techniques for fabrication of highly porous metal nano-structured materials of tuned nanoscale pore morphology and chemistry to make significant technological breakthroughs and hence provide sustainable solutions to the purification of industrial liquid wastes.

Table 2 Application of porous metal membranes in purification technologies

Application	Structure or manufacturer	Main features
Denitrification	Gamma-alumina, zirconia supported Pd, Cu and Pd:Cu alloys particles  (20 to 100 nm)	Catalytic degradation  Highest catalytic activity for 1:1 Pd:Cu alloys <sup>287, 289, 297-299</sup>
Ammonia and phosphate removal	Hitachi Metal  (pore size around 100 nm)	Surface activation  Ozonation lead to lower surface fouling (less than 5 % flux loss in 200 h) <sup>290</sup>
Rainwater purification	FibreTech  (pore size between 1 and 5 µm)	Anti-bacterial effect  Better bacteria (coliform) inactivation than polymeric membranes under ozone for higher flux and lower trans-membrane pressure <sup>300</sup>
Fouling control in microfiltration for municipal sewage reclamation	Hitachi  (pore size around 200 nm)	Intermittent back ozonation more efficient than aeration due to the metal catalytic activity: flux recovery up to 90% after (0.25 mg O <sub>3</sub> .cm <sup>-3</sup> .cycle <sup>-1</sup> ) <sup>301</sup>
Natural Organic Matter removal for colour and TOC removal  MF with coagulation pre-treatment	Hitachi Metal Huber  (pore size between 100 -200 nm)	Full recovery after backwash, no degradation; more than 95% removed after 3 cycles (between 2 cleaning processes)  Coagulation pre-treatment with polyaluminium chloride (PAX-16) of raw water with a colour of 50 mg/L Pt revealed that a specific aluminium dosage of 5 mg/L Al removed >95% of true colour, ~87% of UV-absorbing compounds, and 65–75% of DOC <sup>251, 272</sup>

## **5. Conclusions and prospects**

Porous metal frameworks have unparalleled potential in a number of engineering fields for their versatile catalytic, electrical and mechanical properties. The potentially large range of porous morphologies that can be processed make porous metal frameworks highly promising and complementary alternatives to polymeric and ceramic based materials for sensing, energy storage and molecular separation. Despite being less studied than polymers and ceramics, metal surfaces offer great prospects in terms of functional group coordinating or grafting, leading to a versatile array of potential chemistries. The range of stable coordinated or covalent functional groups that can be linked to pure metal or metal oxide surfaces opens the route to fine tuning for selective adsorption, surface energy interface control and biocompatibility. Novel fabrication and functionalization routes may open the way to the fabrication of porous nanoscale metal materials more economic and reduce capital and maintenance costs for specialty membranes. The development of cheaper nano porous metal frameworks based on easily up-scalable techniques would allow porous metal frameworks to expand their scope of technical applications beyond their mainstream applications of bio-compatible and electrode materials, and target niche markets in water treatment and energy storage.

It appears that novel nano-fabrication techniques, such as de-alloying, electroless depositions, as well as self-assembly of metal NPs are very promising for the preparation of nano-scale pore materials. However, issues related to the stability of the metal NP network and coalescence are however limiting their expansion. Further research is therefore needed in order to design novel fabrication routes or to combine existing approaches, such as electrical sintering or electro-plating with foaming or sintering, in order to better control the interactions between the particles and the inter-connection mechanisms.

## 6. References

1. K. Lauch and W. Ruppert, *Physikalische Zeitschrift*, 1926, **27**, 452-454.
2. T. A. Barr, *Physical Review*, 1952, **87**, 171-171.
3. J. Zhang and W. Liu, *Journal of Membrane Science*, 2011, **371**, 197-210.
4. E. B. Buchanan and J. L. Seago, *J. Electrochem. Soc.*, 1967, **114**, 595-&.
5. D. Borissov, S. Isik-Uppenkamp and M. Rohwerder, *The Journal of Physical Chemistry C*, 2009, **113**, 3133-3138.
6. L. Forget, F. Wilwers, J. Delhalle and Z. Mekhalif, *Appl. Surf. Sci.*, 2003, **205**, 44-55.
7. A. Kloke, C. Köhler, R. Gerwig, R. Zengerle and S. Kerzenmacher, *Advanced Materials*, 2012, **24**, 2916-2921.
8. X. J. Wang, Y. C. Li, P. D. Hodgson and C. Wen, *Tissue Eng. Part A*, 2010, **16**, 309-316.
9. F. Variola, F. Vetrone, L. Richert, P. Jedrzejowski, J. H. Yi, S. Zalzal, S. Clair, A. Sarkissian, D. F. Perepichka, J. D. Wuest, F. Rosei and A. Nanci, *Small*, 2009, **5**, 996-1006.
10. R. Artzi-Gerlitz, K. D. Benkstein, D. L. Lahr, J. L. Hertz, C. B. Montgomery, J. E. Bonevich, S. Semancik and M. J. Tarlov, *Sens. Actuator B-Chem.*, 2009, **136**, 257-264.
11. Y. Ding, Y. J. Kim and J. Erlebacher, *Advanced Materials*, 2004, **16**, 1897-+.
12. L.-X. Qin, Y. Li, D.-W. Li, C. Jing, B.-Q. Chen, W. Ma, A. Heyman, O. Shoseyov, I. Willner, H. Tian and Y.-T. Long, *Angewandte Chemie International Edition*, 2012, **51**, 140-144.
13. M. Wirtz, M. Parker, Y. Kobayashi and C. R. Martin, *Chem Rec*, 2002, **2**, 259-267.
14. C. Li, E. T. Thostenson and T.-W. Chou, *Composites Science and Technology*, 2008, **68**, 1227-1249.
15. L. J. Gibson, *Annual Review of Materials Science*, 2000, **30**, 191-227.
16. Z. Xi, J. Zhu, H. Tang, Q. Ao, H. Zhi, J. Wang and C. Li, *Materials*, 2011, **4**, 816-824.
17. N. Babcsán, J. Banhart and D. Leitlmeier, in *TARTALOM*, Hungary, 2005.
18. J. Banhart, *Prog. Mater. Sci.*, 2001, **46**, 559-U553.
19. J. Banhart, *Journal of Metals*, 2000, **52**, 6.
20. J. Banhart and J. Baumeister, *J. Mater. Sci.*, 1998, **33**, 1431-1440.
21. A. Bhattacharya, V. V. Calmidi and R. L. Mahajan, *Int. J. Heat Mass Transf.*, 2002, **45**, 1017-1031.
22. J. P. Drolet, *International Journal of Powder Metallurgy*, 1977, **13**.
23. A. Jinnapat and A. Kennedy, *Metals*, 2011, **1**, 49-64.
24. S. B. Kulkarni and P. Ramakrishnan, *International Journal of Powder Metallurgy*, 1973, **9**.
25. B. C. Tappan, M. H. Huynh, M. A. Hiskey, D. E. Chavez, E. P. Luther, J. T. Mang and S. F. Son, *Journal of the American Chemical Society*, 2006, **128**, 6589-6594.
26. W. Liu and N. Canfield, *Journal of Membrane Science*, 2012, **409–410**, 113-126.
27. M. A. Asoro, D. Kovar, Y. Shao-Horn, L. F. Allard and P. J. Ferreira, *Nanotechnology*, 2010, **21**, 3.
28. C. T. Campbell, S. C. Parker and D. E. Starr, *Science*, 2002, **298**, 811-814.
29. M. W. J. Luiten-Olieman, L. Winnubst, A. Nijmeijer, M. Wessling and N. E. Benes, *Journal of Membrane Science*, 2011, **370**, 124-130.
30. E. Olevsky and A. Molinari, *International Journal of Plasticity*, 2000, **16**, 1-37.
31. P. S. Liu and K. M. Liang, *J. Mater. Sci.*, 2001, **36**, 5059-5072.
32. M.-A. Neouze and U. Schubert, *Monatshefte für Chemie - Chemical Monthly*, 2008, **139**, 183-195.
33. N. J. Pinto, P. Carrión and J. X. Quiñones, *Materials Science and Engineering: A*, 2004, **366**, 1-5.
34. G. K. Strukova, G. V. Strukov, V. V. Kedrov, I. K. Bdikin and S. A. Zver'kov, *Metal finishing*, 2004.
35. L. Velleman, J. G. Shapter and D. Losic, *Journal of Membrane Science*, 2009, **328**, 121-126.

36. H. Arora, Z. Li, H. Sai, M. Kamperman, S. C. Warren and U. Wiesner, *Macromolecular Rapid Communications*, 2010, **31**, 1960-1964.
37. Y. Wang, C. He, W. Xing, F. Li, L. Tong, Z. Chen, X. Liao and M. Steinhart, *Advanced Materials*, 2010, **22**, 2068-2072.
38. S. C. Warren, L. C. Messina, L. S. Slaughter, M. Kamperman, Q. Zhou, S. M. Gruner, F. J. DiSalvo and U. Wiesner, *Science*, 2008, **320**, 1748-1752.
39. J. C. Thorp, K. Sieradzki, L. Tang, P. A. Crozier, A. Misra, M. Nastasi, D. Mitlin and S. T. Picraux, *Applied Physics Letters*, 2006, **88**, 033110-033113.
40. A. Abrutis, A. Bartasyte, G. Garcia, A. Teiserskis, V. Kubilius, Z. Saltyte, V. Faucheu, A. Figueras and S. Rushworth, *Thin Solid Films*, 2004, **449**, 94-99.
41. T. Ikeda and H. Nakajima, *Materials Letters*, 2004, **58**, 3807-3811.
42. G. Xomeritakis and Y. S. Lin, *Journal of Membrane Science*, 1996, **120**, 261-272.
43. D. G. Anderson, N. Anwar, B. J. Aylett, L. G. Earwaker, M. I. Nasir, J. P. G. Farr, K. Stiebahl and J. M. Keen, *Journal of Organometallic Chemistry*, 1992, **437**, C7-C12.
44. K. Daub, V. K. Wunder and R. Dittmeyer, *Catalysis Today*, 2001, **67**, 257-272.
45. C. A. Scholes, K. H. Smith, S. E. Kentish and G. W. Stevens, *International Journal of Greenhouse Gas Control*, 2010, **4**, 739-755.
46. J. H. Tong, C. L. Su, K. Kuraoka, H. Suda and Y. Matsumura, *Journal of Membrane Science*, 2006, **269**, 101-108.
47. K. Zhang, H. Y. Gao, Z. B. Rui, P. Liu, Y. D. Li and Y. S. Lin, *Ind. Eng. Chem. Res.*, 2009, **48**, 1880-1886.
48. S. Byun, S. H. Davies, A. L. Alpatova, L. M. Corneal, M. J. Baumann, V. V. Tarabara and S. J. Masten, *Water Research*, 2011, **45**, 163-170.
49. L.-C. Cheng, J.-H. Huang, H. M. Chen, T.-C. Lai, K.-Y. Yang, R.-S. Liu, M. Hsiao, C.-H. Chen, L.-J. Her and D. P. Tsai, *Journal of Materials Chemistry*, 2012, **22**, 2244-2253.
50. W. Y. Choi, J. Chung, C. H. Cho and J. O. Kim, *Desalination*, 2011, **279**, 359-366.
51. K. Jong-Oh, J. Jong-Tae and C. Won-Youl, *Key Eng. Mater.*, 2006, **236-328**, 1317-13201320.
52. J. Jong-Tae, K. Jong-Oh and C. Won-Youl, *Mater. Sci. Forum*, 2008, **569**, 5-88.
53. J. Kováčik and F. Simančík, in *MetFoam '99*, ed. MetalFoam.net, Bremen, Germany, 1999.
54. Z. Hua, Y. Deng, K. Li and S. Yang, *Nanoscale Research Letters*, 2012, **7**, 129.
55. B. C. Tappan, S. A. Steiner and E. P. Luther, *Angewandte Chemie International Edition*, 2010, **49**, 4544-4565.
56. J. R. Groza, *Nanostructured Materials*, 1999, **12**, 987-992.
57. I. Vida-Simiti, N. Jumate, G. Thalmaier, N. Sechel and V. Moldovan, *Journal of Porous Materials*, 2012, **19**, 21-27.
58. Y. Tang, H. T. Loh, Y. S. Wong, J. Y. H. Fuh, L. Lu and X. Wang, *Journal of Materials Processing Technology*, 2003, **140**, 368-372.
59. W. O'Neill, C. J. Sutcliffe, R. Morgan, A. Landsborough and K. K. B. Hon, *CIRP Annals - Manufacturing Technology*, 1999, **48**, 151-154.
60. R. Orrù, R. Licheri, A. M. Locci, A. Cincotti and G. Cao, *Materials Science and Engineering: R: Reports*, 2009, **63**, 127-287.
61. E. Füglein and K. Ott, The Correlation between Particle Size and Sintering Temperature using Barium Titanate (BaTiO<sub>3</sub>) as an Example, [http://www.netzsch-thermal-analysis.com/uploads/ttx\\_nxnetzschmedia/files/316\\_allgemein.pdf](http://www.netzsch-thermal-analysis.com/uploads/ttx_nxnetzschmedia/files/316_allgemein.pdf), Accessed 15 March 2013, 2013.
62. I. Vida-Simiti, N. Jumate, G. Thalmaier, N. Sechel and V. Moldovan, *Environmental Engineering & Management Journal (EEMJ)*, 2011, **10**, 1439-1444.
63. L. A. Mark, A. Mikko, M. Tomi, A. Ari, O. Kimmo, S. Mika and S. Heikki, *Nanotechnology*, 2008, **19**, 175201.
64. M. Hummelgård, R. Zhang, H.-E. Nilsson and H. Olin, *PLoS ONE*, 2011, **6**, e17209.

65. I. Reinhold, C. E. Hendriks, R. Eckardt, J. M. Kranenburg, J. Perelaer, R. R. Baumann and U. S. Schubert, *Journal of Materials Chemistry*, 2009, **19**, 3384-3388.
66. N. R. Denny, F. Li, D. J. Norris and A. Stein, *Journal of Materials Chemistry*, 2010, **20**, 1538-1545.
67. J. W. Kim, S. H. Kim, S. Y. Song and Y. D. Kim, *J. Appl. Phys.*, 2012, **111**, 07A720-723.
68. M. Mota, J. Teixeira, A. Yelshin and S. Cortez, *Journal of chromatography. B, Analytical technologies in the biomedical and life sciences*, 2006, **843**, 63-72.
69. T. Suteewong, H. Sai, R. Hovden, D. Muller, M. S. Bradbury, S. M. Gruner and U. Wiesner, *Science*, 2013, **340**, 337-341.
70. A. S. Verkman, *Annual Review of Medicine*, 2012, **63**, 303-316.
71. A. S. Verkman and A. K. Mitra, *American Journal of Physiology - Renal Physiology*, 2000, **278**, F13-F28.
72. S. Venkataraman, J. L. Hedrick, Z. Y. Ong, C. Yang, P. L. Ee, P. T. Hammond and Y. Y. Yang, *Advanced drug delivery reviews*, 2011, **63**, 1228-1246.
73. S. Magdassi, M. Grouchko, O. Berezin and A. Kamyshny, *ACS Nano*, 2010, **4**, 1943-1948.
74. S. H. Ko, J. Chung, N. Hotz, K. H. Nam and C. P. Grigoropoulos, *Journal of Micromechanics and Microengineering*, 2010, **20**, 125010.
75. D. Kim, S. Jeong, J. Moon, S. Han and J. Chung, *Applied Physics Letters*, 2007, **91**, 071114-071113.
76. T. Öhlund, J. Örtegren, S. Forsberg and H.-E. Nilsson, *Appl. Surf. Sci.*, 2012, **259**, 731-739.
77. S. S. Madaeni, M. E. Aalami-Aleagha and P. Daraei, *Journal of Membrane Science*, 2008, **320**, 541-548.
78. G. Erskine, Steri-Flow Filtration Systems (Aust) Pty Ltd, Australia, 2011.
79. V. K. Rangari, G. M. Mohammad, S. Jeelani, A. Hundley, K. Vig, S. R. Singh and S. Pillai, *Nanotechnology*, 2010, **21**, 095102.
80. G. Schmid and D. Fenske, *Philosophical Transactions of the Royal Society A: Mathematical, Physical and Engineering Sciences*, 2010, **368**, 1207-1210.
81. W.-J. Jin, H. K. Lee, E. H. Jeong, W. H. Park and J. H. Youk, *Macromolecular Rapid Communications*, 2005, **26**, 1903-1907.
82. R. D. Haghghi, S. A. J. Jahromi, A. Moresedgh and M. T. Khorshid, *J. of Materi Eng and Perform*, 2012, **21**, 1885-1892.
83. I. M. Fedorchenko and A. G. Kostornov, *Powder Metall Met Ceram*, 1966, **5**, 366-369.
84. S. Ahmad, N. Muhamad, A. Muchtar, J. Sahari, K. R. Jamaludin, M. H. I. Ibrahim, N. H. Mohamad Nor and I. Murtadahahadi, in *Brunei International Conference of Engineering and Technology (BICET) 2008*, Brunei, 2008.
85. J. Babcsán Kiss, A. Berthold, N. Babcsán and H. Schubert, in *MetFoam 2005 Kyoto Japan*, 2005.
86. L. Dumeer, L. Velleman, K. Sears, M. Hill, J. Schutz, N. Finn, M. Duke and S. Gray, *Membranes*, 2010, **1**, 25-36.
87. R. Bhandari and Y. H. Ma, *Journal of Membrane Science*, 2009, **334**, 50-63.
88. C. R. Martin, V. P. Menon and M. Nishizawa, *Science*, 1995, **268**, 700+.
89. V. P. Menon and C. R. Martin, *Analytical Chemistry*, 1995, **67**, 1920-1928.
90. P. Tierno and W. A. Goedel, *The Journal of Physical Chemistry B*, 2006, **110**, 3043-3050.
91. S. C. Domenech, E. Lima Jr, V. Drago, J. C. De Lima, N. G. Borges Jr, A. O. V. Avila and V. Soldi, *Appl. Surf. Sci.*, 2003, **220**, 238-250.
92. S.-M. Hwang, J.-H. Lim, C.-M. Lee, E.-C. Park, J.-H. Choi, J. Joo, H.-J. Lee and S.-B. Jung, *Transactions of Nonferrous Metals Society of China*, 2009, **19**, 970-974.
93. M. Šimor, J. Ráhel', M. Černák, Y. Imahori, M. Štefečka and M. Kando, *Surface and Coatings Technology*, 2003, **172**, 1-6.
94. S.-Y. Cheon, S.-Y. Park, Y.-M. Rhym, D.-H. Kim and J.-H. Lee, *Current Applied Physics*, 2011, **11**, 790-793.

95. Z. Wu, S. Ge, M. Zhang, W. Li and K. Tao, *Journal of Colloid and Interface Science*, 2009, **330**, 359-366.
96. L. Dumee, M. R. Hill, M. Duke, L. Velleman, K. Sears, J. Schutz, N. Finn and S. Gray, *J. Mater. Chem.*, 2012, **22**, 9374-9378.
97. J. Hu, W. Li, J. Chen, X. Zhang and X. Zhao, *Surface and Coatings Technology*, 2008, **202**, 2922-2926.
98. E. Delamarche, J. Vichiconti, S. A. Hall, M. Geissler, W. Graham, B. Michel and R. Nunes, *Langmuir*, 2003, **19**, 6567-6569.
99. S. K. Ryi, J. S. Park, S. H. Choi, S. H. Cho and S. H. Kim, *Separation and Purification Technology*, 2006, **47**, 148-155.
100. L. Velleman, D. Losic and J. G. Shapter, *Journal of Membrane Science*, 2012.
101. Y. Kobayashi, Y. Tadaki, D. Nagao and M. Konno, *Journal of Colloid and Interface Science*, 2005, **283**, 601-604.
102. R. P. Hodson, A. E. Strevens and A. Drury, in *Opto-Ireland 2005: Nanotechnology and Nanophotonics*, eds. W. J. Blau, D. Kennedy and J. Colreavy, Spie-Int Soc Optical Engineering, Bellingham, 2005, pp. 114-122.
103. M.-C. Huang, T.-L. Chang, T.-H. Kao and C.-C. Fu, *Microsyst Technol*, 2013, **19**, 455-460.
104. M. A. Bromley and C. Boxall, *ECS Transactions*, 2013, **53**, 123-132.
105. L. Woo, F. Hong Jin, M. Alexe, R. Scholz, M. Zacharias, K. Nielsch and U. Gösele, in *Nanotechnology Materials and Devices Conference, 2006. NMDC 2006. IEEE*, 2006, pp. 306-307.
106. W. Lee, M. Alexe, K. Nielsch and U. Gösele, *Chemistry of Materials*, 2005, **17**, 3325-3327.
107. J. Rebelli, A. A. Rodriguez, S. Ma, C. T. Williams and J. R. Monnier, *Catalysis Today*, 2011, **160**, 170-178.
108. J. B. Liu, W. Dong, P. Zhan, S. Z. Wang, J. H. Zhang and Z. L. Wang, *Langmuir*, 2005, **21**, 1683-1686.
109. I. Ron, N. Friedman, D. Cahen and M. Sheves, *Small*, 2008, **4**, 2271-2278.
110. R. J. Gilliam, S. J. Thorpe and D. W. Kirk, *J Appl Electrochem*, 2007, **37**, 233-239.
111. L. Velleman, J.-L. Bruneel, F. Guillaume, D. Losic and J. G. Shapter, *Physical Chemistry Chemical Physics*, 2011, **13**, 19587-19593.
112. D. H. Reneker and I. Chun, *Nanotechnology*, 1996, **7**, 216-223.
113. Z. M. Huang, Y. Z. Zhang, M. Kotaki and S. Ramakrishna, *Composites Science and Technology*, 2003, **63**, 2223-2253.
114. D. Li and Y. N. Xia, *Advanced Materials*, 2004, **16**, 1151-1170.
115. D. Li and Y. N. Xia, *Nano Lett.*, 2003, **3**, 555-560.
116. H. Wu, R. Zhang, X. Liu, D. Lin and W. Pan, *Chemistry of Materials*, 2007, **19**, 3506-3511.
117. H. Wu, L. Hu, M. W. Rowell, D. Kong, J. J. Cha, J. R. McDonough, J. Zhu, Y. Yang, M. D. McGehee and Y. Cui, *Nano Lett.*, 2010, **10**, 4242-4248.
118. C. L. Shao, H. Y. Guan, Y. C. Liu, J. Gong, N. Yu and X. H. Yang, *Journal of Crystal Growth*, 2004, **267**, 380-384.
119. H. Y. Guan, C. L. Shao, Y. C. Liu, N. Yu and X. H. Yang, *Solid State Communications*, 2004, **131**, 107-109.
120. D. Li and Y. Xia, *Nano Lett.*, 2004, **4**, 933-938.
121. M. Macías, A. Chacko, J. P. Ferraris and K. J. Balkus Jr, *Microporous and Mesoporous Materials*, 2005, **86**, 1-13.
122. C. C. Doumanidis, *Microelectronic Engineering*, 2009, **86**, 467-478.
123. K. J. Senecal, D. P. Ziegler, J. N. He, R. Mosurkal, H. Schreuder-Gibson and L. A. Samuelson, in *Organic Optoelectronic Materials, Processing and Devices*, ed. S. C. Moss, Materials Research Society, Warrendale, 2002, pp. 285-289.
124. L. Song, S. Liu, Q. Lu and G. Zhao, *Appl. Surf. Sci.*, 2012, **258**, 3789-3794.
125. S. Swaminathan and G. Chase, ed. InTech, 2011.

126. N. S. Hansen, D. Cho and Y. L. Joo, *Small*, 2012, **8**, 1510-1514.
127. N. A. M. Barakat, B. Kim and H. Y. Kim, *The Journal of Physical Chemistry C*, 2008, **113**, 531-536.
128. M. Bognitzki, M. Becker, M. Graeser, W. Massa, J. H. Wendorff, A. Schaper, D. Weber, A. Beyer, A. Gölzhäuser and A. Greiner, *Advanced Materials*, 2006, **18**, 2384-2386.
129. C. D. Saquing, J. L. Manasco and S. A. Khan, *Small*, 2009, **5**, 944-951.
130. N. E. Shi, J. J. Duan, J. Su, F. Z. Huang, W. Xue, C. Zheng, Y. Qian, S. F. Chen, L. H. Xie and W. Huang, *J. Appl. Polym. Sci.*, 2013, **128**, 1004-1010.
131. S. K. Ryi, J. S. Park, S. H. Kim, S. H. Cho and D. W. Kim, *Journal of Membrane Science*, 2006, **279**, 439-445.
132. K. Alexander, S. Joachim and M. Shlomo, *The Open Applied Physics Journal of Aerosol Science*, 2011, **4**, 17.
133. T. W. Hansen, A. T. Delariva, S. R. Challa and A. K. Datye, *Acc Chem Res*, 2013.
134. C. T. Campbell, *Accounts of Chemical Research*, 2013.
135. S. C. Warren, M. R. Perkins, A. M. Adams, M. Kamperman, A. A. Burns, H. Arora, E. Herz, T. Suteewong, H. Sai, Z. Li, J. Werner, J. Song, U. Werner-Zwanziger, J. W. Zwanziger, M. Grätzel, F. J. DiSalvo and U. Wiesner, *Nat Mater*, 2012, **11**, 460-467.
136. Z. Li, H. Sai, S. C. Warren, M. Kamperman, H. Arora, S. M. Gruner and U. Wiesner, *Chemistry of Materials*, 2009, **21**, 5578-5584.
137. J. N. L. Albert and T. H. Epps III, *Materials Today*, 2010, **13**, 24-33.
138. Y. Mai and A. Eisenberg, *Chemical Society Reviews*, 2012, **41**, 5969-5985.
139. G. Riess, *Progress in Polymer Science*, 2003, **28**, 1107-1170.
140. H.-S. Jang, T.-H. Kim, C. Do, M.-J. Lee and S.-M. Choi, *Soft Matter*, 2013, **9**, 3050-3056.
141. B. Platschek, N. Petkov, D. Himsel, S. Zimdars, Z. Li, R. Köhn and T. Bein, *Journal of the American Chemical Society*, 2008, **130**, 17362-17371.
142. W. Kubo, M. Takahashi, K. Okamoto, S. Kitamura and H. Miyata, *Langmuir*, 2013.
143. P. R. Desai, N. J. Jain, R. K. Sharma and P. Bahadur, *Colloids and Surfaces A: Physicochemical and Engineering Aspects*, 2001, **178**, 57-69.
144. D. Gross, A. R. Balkenende, P. A. Albouy, A. Ayral, H. Amenitsch and F. Babonneau, *Chemistry of Materials*, 2001, **13**, 1848-1856.
145. S. C. Warren, L. C. Messina, L. S. Slaughter, M. Kamperman, Q. Zhou, S. M. Gruner, F. J. DiSalvo and U. Wiesner, *Science*, 2008, **320**, 1748-1752.
146. T. Sakai and P. Alexandridis, *The Journal of Physical Chemistry B*, 2005, **109**, 7766-7777.
147. D. M. Dotzauer, J. H. Dai, L. Sun and M. L. Bruening, *Nano Lett.*, 2006, **6**, 2268-2272.
148. A. V. Khoryushin, P. B. Mozhaev, J. E. Mozhaeva, I. K. Bdikin, Y. Zhao, N. H. Andersen, C. S. Jacobsen and J. B. Hansen, *Physica C: Superconductivity*, 2013, **486**, 1-8.
149. S. Weinkauf and L. Bachmann, *Ultramicroscopy*, 1992, **46**, 113-134.
150. P. Jian, H. Yahui, W. Yang and L. Linlin, *Journal of Membrane Science*, 2006, **284**, 9-16.
151. L. Ouyang, D. M. Dotzauer, S. R. Hogg, J. Macanás, J.-F. Lahitte and M. L. Bruening, *Catalysis Today*, 2010, **156**, 100-106.
152. D. M. Dotzauer, J. Dai, L. Sun and M. L. Bruening, *Nano Lett.*, 2006, **6**, 2268-2272.
153. F. Xiao, *The Journal of Physical Chemistry C*, 2012, **116**, 16487-16498.
154. S. B. Fuller, E. J. Wilhelm and J. M. Jacobson, *Microelectromechanical Systems, Journal of*, 2002, **11**, 54-60.
155. G. C. Jensen, C. E. Krause, G. A. Sotzing and J. F. Rusling, *Physical chemistry chemical physics : PCCP*, 2011, **13**, 4888-4894.
156. J. Rausch, L. Salun, S. Griesheimer, M. Ibis and R. Werthschützky, in *SENSOR & TEST Conference*, Nürnberg, Germany, 2011.
157. H. Zhang, A. Xie, Y. Shen, L. Qiu and X. Tian, *Physical chemistry chemical physics : PCCP*, 2012, **14**, 12757-12763.

158. D. L. Guo, X. Huang, G. Z. Xing, Z. Zhang, G. P. Li, M. He, H. Zhang, H. Chen and T. Wu, *Physical Review B*, 2011, **83**, 045403.
159. W. Shen, M. Li, C. Ye, L. Jiang and Y. Song, *Lab on a Chip*, 2012, **12**, 3089-3095.
160. K. Abe, K. Suzuki and D. Citterio, *Analytical Chemistry*, 2008, **80**, 6928-6934.
161. H. W. Pickering, *J Electrochem Soc*, 1970, **117**, 8-15.
162. C. Zhao, Z. Qi, X. Wang and Z. Zhang, *Corros Sci*, 2009, **51**, 2120-2125.
163. W. Yeh and S. Chava, *Journal of Vacuum Science & Technology B: Microelectronics and Nanometer Structures*, 2009, **27**, 923-927.
164. L. H. Qian and M. W. Chen, *Applied Physics Letters*, 2007, **91**, 083105-083103.
165. D. J. Wang, Z. H. Li, M. A. Rahman and J. Shen, *Langmuir*, 2013, **29**, 8108-8115.
166. N. A. Senior and R. C. Newman, *Nanotechnology*, 2006, **17**, 2311.
167. X.-l. Tan, K. Li, G. Niu, Z. Yi, J.-s. Luo, Y. Liu, S.-j. Han, W.-d. Wu and Y.-j. Tang, *J. Cent. South Univ. Technol.*, 2012, **19**, 17-21.
168. G. W. Nyce, J. R. Hayes, A. V. Hamza and J. H. Satcher, *Chemistry of Materials*, 2007, **19**, 344-346.
169. B. CHEUNG, 2010.
170. L.-Y. Chen, J.-S. Yu, T. Fujita and M.-W. Chen, *Advanced Functional Materials*, 2009, **19**, 1221-1226.
171. L. Sun, C.-L. Chien and P. C. Searson, *Chemistry of Materials*, 2004, **16**, 3125-3129.
172. R. Li and K. Sieradzki, *Phys Rev Lett*, 1992, **68**, 1168-1171.
173. A. Wonisch, T. Kraft, M. Moseler and H. Riedel, *Journal of the American Ceramic Society*, 2009, **92**, 1428-1434.
174. V. V. Skorokhod, O. I. Get'man, A. E. Zuev and S. P. Rakitin, *Powder Metall Met Ceram*, 1988, **27**, 941-947.
175. F. Sánchez, A. M. Bolarín, P. Molera, J. E. Mendoza and M. Ocampo, *Rev. LatinAm. Met. Mat.*, 2003, **23**.
176. D. Brodoceanu, C. Fang, N. H. Voelcker, C. T. Bauer, A. Wonn, E. Kroner, E. Arzt and T. Kraus, *Nanotechnology*, 2013, **24**, 085304.
177. S. E. H. Murph, S. M. Serkiz, E. B. Fox, H. Colon-Mercado, L. Sexton and M. Siegfried, in *Fluorine-Related Nanoscience with Energy Applications*, eds. D. J. Nelson and C. N. Brammer, Amer Chemical Soc, Washington, 2010, pp. 127-163.
178. D. L. Feldheim and C. A. J. Foss, *Metal nanoparticles: synthesis, characterization, and applications*, CRC Press, New York, 2002.
179. R. K. Singh Raman, P. Chakraborty Banerjee, D. E. Lobo, H. Gullapalli, M. Sumandasa, A. Kumar, L. Choudhary, R. Tkacz, P. M. Ajayan and M. Majumder, *Carbon*, 2012, **50**, 4040-4045.
180. J. L. H. Chau, C.-Y. Chen and C.-C. Yang, *Arabian Journal of Chemistry*, 2013.
181. B. Pukanszky and E. Fekete, in *Advances in Polymer Science; Mineral fillers in thermoplastics, I. Raw materials and processing*, ed. J. Jancar, Springer-Verlag, Heidelberger Platz 3, D-1000 Berlin, Germany; Springer-Verlag New York, Inc., 175 Fifth Avenue, New York, New York 10010, USA, 1999, pp. 109-153.
182. S. G. Grancharov, H. Zeng, S. Sun, S. X. Wang, S. O'Brien, C. B. Murray, J. R. Kirtley and G. A. Held, *J Phys Chem B*, 2005, **109**, 13030-13035.
183. P. Raveendran, J. Fu and S. L. Wallen, *Journal of the American Chemical Society*, 2003, **125**, 13940-13941.
184. A. A. Gromov, Y. I. Strokova and U. Teipel, *Chemical Engineering & Technology*, 2009, **32**, 1049-1060.
185. B. C. Sih and M. O. Wolf, *Chem Commun*, 2005, **21**, 3375-3384.
186. Z. Guan, L. Polavarapu and Q.-H. Xu, *Langmuir*, 2010, **26**, 18020-18023.
187. E. Casals, T. Pfaller, A. Duschl, G. J. Oostingh and V. F. Puntes, *Small*, 2011, **7**, 3479-3486.
188. J. M. Galloway and S. S. Staniland, *Journal of Materials Chemistry*, 2012, **22**, 12423-12434.

189. S. Si, M. Raula, T. K. Paira and T. K. Mandal, *Chemphyschem*, 2008, **9**, 1578-1584.
190. P. Free, D. Paramelle, M. Bosman, J. Hobley and D. G. Fernig, *Australian Journal of Chemistry*, 2012, **65**, 275-282.
191. C. Kirchner, M. George, B. Stein, W. J. Parak, H. E. Gaub and M. Seitz, *Advanced Functional Materials*, 2002, **12**, 266-276.
192. D. Wan, S. Yuan, K. G. Neoh and E. T. Kang, *ACS Appl Mater Interfaces*, 2010, **2**, 1653-1662.
193. E. Rampazzo, E. Brasola, S. Marcuz, F. Mancin, P. Tecilla and U. Tonellato, *Journal of Materials Chemistry*, 2005, **15**, 2687-2696.
194. K. V. Rajkumar, S. Vaidyanathan, A. Kumar, T. Jayakumar, B. Raj and K. K. Ray, *Journal of Magnetism and Magnetic Materials*, 2007, **312**, 359-365.
195. Z. Q. Mao, Z. H. He, D. H. Chen, W. Y. Cheung and S. P. Wong, *Solid State Communications*, 2007, **142**, 329-332.
196. F. M. Liu, B. F. Quan, Z. Q. Liu and L. H. Chen, *Materials Chemistry and Physics*, 2005, **93**, 301-304.
197. Z. Elbhiri, Y. Chevalier, J. M. Chovelon and N. Jaffrezic-Renault, *Talanta*, 2000, **52**, 495-507.
198. F. J. Hua, M. T. Swihart and E. Ruckenstein, *Langmuir*, 2005, **21**, 6054-6062.
199. G. Eilers, C. Zettersten, L. Nyholm, L. Hammarstrom and R. Lomoth, *Dalton Trans*, 2005, **21**, 1033-1041.
200. A. Ulman, *Chem Rev*, 1996, **96**, 1533-1554.
201. Q. L. Zhang, L. C. Du, Y. X. Weng, L. Wang, H. Y. Chen and J. Q. Li, *Journal of Physical Chemistry B*, 2004, **108**, 15077-15083.
202. S. W. Schmidt, T. Christ, C. Glockner, M. K. Beyer and H. Clausen-Schaumann, *Langmuir*, 2010, **26**, 15333-15338.
203. L. M. Bishop, J. C. Yeager, X. Chen, J. N. Wheeler, M. D. Torelli, M. C. Benson, S. D. Burke, J. A. Pedersen and R. J. Hamers, *Langmuir*, 2012, **28**, 1322-1329.
204. G. Kickelbick and U. Schubert, in *Synthesis, Functionalization and Surface Treatment of Nanoparticles*, ed. B. M.I., 2003, p. 91.
205. J. H. Moon, Y. G. Shul, H. S. Han, S. Y. Hong, Y. S. Choi and H. T. Kim, *International Journal of Adhesion and Adhesives*, 2005, **25**, 301-312.
206. A. del Campo, T. Sen, J. P. Lelouche and I. J. Bruce, *Journal of Magnetism and Magnetic Materials*, 2005, **293**, 33-40.
207. T. Kikukawa, K. Kuraoka, K. Kawabe, M. Yamashita, K. Fukumi, K. Hirao and T. Yazawa, *Journal of Membrane Science*, 2005, **259**, 161-166.
208. E. Pere, H. Cardy, V. Latour and S. Lacombe, *Journal of Colloid and Interface Science*, 2005, **281**, 410-416.
209. S. Reculusa, C. Poncet-Legrand, A. Perro, E. Duguet, E. Bourgeat-Lami, C. Mingotaud and S. Ravaine, *Chemistry of Materials*, 2005, **17**, 3338-3344.
210. R. De Palma, S. Peeters, M. J. Van Bael, H. Van den Rul, K. Bonroy, W. Laureyn, J. Mullens, G. Borghs and G. Maes, *Chemistry of Materials*, 2007, **19**, 1821-1831.
211. C. Haensch, S. Hoeppener and U. S. Schubert, *Chemical Society Reviews*, 2010, **39**, 2323-2334.
212. T. Baumgärtel, C. von Borczyskowski and H. Graaf, *Beilstein Journal of Nanotechnology*, 2013, **4**, 218-226.
213. N. Adden, L. J. Gamble, D. G. Castner, A. Hoffmann, G. Gross and H. Menzel, *Langmuir*, 2006, **22**, 8197-8204.
214. P. H. Mutin, G. Guerrero and A. Vioux, *Journal of Materials Chemistry*, 2005, **15**, 3761-3768.
215. M. Chauhan, C. Chuit, A. Fruchier and C. Reye, *Inorganic Chemistry*, 1999, **38**, 1336-1339.
216. A. Subbiah, D. Pyle, A. Rowland, J. Huang, R. A. Narayanan, P. Thiagarajan, J. Zon and A. Clearfield, *Journal of the American Chemical Society*, 2005, **127**, 10826-10827.
217. E. Hoque, J. A. DeRose, G. Kulik, P. Hoffmann, H. J. Mathieu and B. Bhushan, *The Journal of Physical Chemistry B*, 2006, **110**, 10855-10861.

218. M. A. White, J. A. Johnson, J. T. Koberstein and N. J. Turro, *Journal of the American Chemical Society*, 2006, **128**, 11356-11357.
219. G. P. Holland, R. Sharma, J. O. Agola, S. Amin, V. C. Solomon, P. Singh, D. A. Buttry and J. L. Yarger, *Chemistry of Materials*, 2007, **19**, 2519-2526.
220. G. Guerrero, P. H. Mutin and A. Vioux, *Chemistry of Materials*, 2001, **13**, 4367-4373.
221. K. E. Jabalpurwala, K. A. Venkatachalam and M. B. Kabadi, *Journal of Inorganic and Nuclear Chemistry*, 1964, **26**, 1027-1043.
222. G. W. Luther, 3rd, S. M. Theberge and D. Rickard, *Talanta*, 2000, **51**, 11-20.
223. R. C. Doty, T. R. Tshikhudo, M. Brust and D. G. Fernig, *Chemistry of Materials*, 2005, **17**, 4630-4635.
224. S. Roux, B. Garcia, J. L. Bridot, M. Salome, C. Marquette, L. Lemelle, P. Gillet, L. Blum, P. Perriat and O. Tillement, *Langmuir*, 2005, **21**, 2526-2536.
225. M. G. Warner and J. E. Hutchison, in *Synthesis, Functionalization and Surface Treatment of Nanoparticles*, ed. ASP, 2002.
226. E. Ramirez, S. Jansat, K. Philippot, P. Lecante, M. Gomez, A. M. Masdeu-Bultó and B. Chaudret, *Journal of Organometallic Chemistry*, 2004, **689**, 4601-4610.
227. H. Fan, Z. Chen, C. J. Brinker, J. Clawson and T. Alam, *J Am Chem Soc*, 2005, **127**, 13746-13747.
228. G. H. Woehrle, M. G. Warner and J. E. Hutchison, *The Journal of Physical Chemistry B*, 2002, **106**, 9979-9981.
229. P. G. Eller and G. J. Kubas, *Journal of the American Chemical Society*, 1977, **99**, 4346-4351.
230. D. Stalke, *Chem Commun*, 2012, **48**, 9559-9573.
231. T. Y. Dong, H. H. Wu and M. C. Lin, *Langmuir*, 2006, **22**, 6754-6756.
232. P. C. Ohara, D. V. Leff, J. R. Heath and W. M. Gelbart, *Physical Review Letters*, 1995, **75**, 3466-3469.
233. D. Kisailus, M. Najarian, J. C. Weaver and D. E. Morse, *Advanced Materials*, 2005, **17**, 1234-+.
234. P. Jiang, A. Nion, A. Marchenko, L. Piot and D. Fichou, *J Am Chem Soc*, 2006, **128**, 12390-12391.
235. M. J. Hostetler, J. E. Wingate, C. J. Zhong, J. E. Harris, R. W. Vachet, M. R. Clark, J. D. Londono, S. J. Green, J. J. Stokes, G. D. Wignall, G. L. Glish, M. D. Porter, N. D. Evans and R. W. Murray, *Langmuir*, 1998, **14**, 17-30.
236. G. Schmid, *Nanoparticles: From Theory to Application*, Weinheim, 2004.
237. R. Rousseau, V. De Renzi, R. Mazzarello, D. Marchetto, R. Biagi, S. Scandolo and U. del Pennino, *The Journal of Physical Chemistry B*, 2006, **110**, 10862-10872.
238. M. J. Hostetler, A. C. Templeton and R. W. Murray, *Langmuir*, 1999, **15**, 3782-3789.
239. S. Rucareanu, V. J. Gandubert and R. B. Lennox, *Chemistry of Materials*, 2006, **18**, 4674-4680.
240. J. J. Gooding, F. Mearns, W. R. Yang and J. Q. Liu, *Electroanalysis*, 2003, **15**, 81-96.
241. A. B. R. Mayer, *Polymers for Advanced Technologies*, 2001, **12**, 96-106.
242. M. Brust, R. Etchenique, E. J. Calvo and G. J. Gordillo, *Chemical Communications*, 1996, 1949-1950.
243. S. Kolliopoulos, P. Dimitrakis, P. Normand, H. L. Zhang, N. Cant, S. D. Evans, S. Paul, C. Pearson, A. Molloy, M. C. Petty and D. Tsoukalas, *J. Appl. Phys.*, 2003, **94**, 5234-5239.
244. M. Bieri and T. Burgi, *Langmuir*, 2006, **22**, 8379-8386.
245. C. Gautier and T. Burgi, *Chem Commun*, 2005, **21**, 5393-5395.
246. Y. Hu, X. Zhao, Y. J. Huang, Q. F. Li, N. J. Bjerrum, C. P. Liu and W. Xing, *J. Power Sources*, 2013, **225**, 129-136.
247. J. Tian, T. J. Lu, H. P. Hodson, D. T. Queheillalt and H. N. G. Wadley, *Int. J. Heat Mass Transf.*, 2007, **50**, 2521-2536.
248. T. Kim, H. P. Hodson and T. J. Lu, *Int. J. Heat Mass Transf.*, 2004, **47**, 1129-1140.
249. T. Kim, H. P. Hodson and T. J. Lu, *Int. J. Heat Mass Transf.*, 2005, **48**, 4243-4264.

250. C. S. Roper, K. D. Fink, S. T. Lee, J. A. Kolodziejska and A. J. Jacobsen, *AIChE Journal*, 2013, **59**, 622-629.
251. P.-X. Jiang, M. Li, T.-J. Lu, L. Yu and Z.-P. Ren, *Int. J. Heat Mass Transf.*, 2004, **47**, 2085-2096.
252. J. Tian, T. Kim, T. J. Lu, H. P. Hodson, D. T. Queheillalt, D. J. Sypek and H. N. G. Wadley, *Int. J. Heat Mass Transf.*, 2004, **47**, 3171-3186.
253. M. Almajali, K. Lafdi and P. H. Prodhomme, *Energy Conversion and Management*, 2013, **66**, 336-342.
254. R. Neugebauer, H. Brdunlich and U. Wagner, *MRS Online Proceedings Library*, 1998, **521**, null-null.
255. K. U. Kainer, in *Metal Matrix Composites*, Wiley-VCH Verlag GmbH & Co. KGaA, 2006, pp. 1-54.
256. A. P. Technologies, <http://www.appliedporous.com/apps.htm>, Accessed 19/09/2013.
257. Y. Gan, *International Journal of Molecular Sciences*, 2009, **10**, 5115-5134.
258. C. Toscano, C. Meola and G. M. Carlomagno, *Journal of Composites*, 2013, **2013**, 8.
259. W. F. Ding, J. H. Xu, Z. Z. Chen, C. Y. Yang, C. J. Song and Y. C. Fu, *Int J Adv Manuf Technol*, 2013, **67**, 1309-1315.
260. V. Goyal and A. A. Balandin, *Applied Physics Letters*, 2012, **100**, 073113-073114.
261. F. Zok, S. Jansson, A. G. Evans and V. Nardone, *MTA*, 1991, **22**, 2107-2117.
262. ERGAEROSPACE, <http://www.ergaerospace.com/Descriptors.htm>, Accessed 19/09/2013.
263. MOTT, [http://www.mottcorp.com/news/2008\\_11\\_Aerospace.cfm](http://www.mottcorp.com/news/2008_11_Aerospace.cfm), Accessed 19/09/2013.
264. M. Tiemann, *Chemistry (Weinheim an der Bergstrasse, Germany)*, 2007, **13**, 8376-8388.
265. L. Yi Jae, O. Cheonseok, P. Jae Yeong and K. Younghun, *Nanotechnology, IEEE Transactions on*, 2011, **10**, 1298-1305.
266. G. Scheen, M. Bassu and L. Francis, *Nanoscale Research Letters*, 2012, **7**, 395.
267. P. M. Biesheuvel, Y. Fu and M. Z. Bazant, *Physical Review E*, 2011, **83**, 061507.
268. L. Hu, H. Wu and Y. Cui, *Mrs Bulletin*, 2011, **36**, 760-765.
269. R. N. Viswanath, *Conference proceedings : ... Annual International Conference of the IEEE Engineering in Medicine and Biology Society. IEEE Engineering in Medicine and Biology Society. Conference*, 2009, **2009**, 6838-6841.
270. J. H. Lee, M. A. Mahmoud, V. Sitterle, J. Sitterle and J. C. Meredith, *J Am Chem Soc*, 2009, **131**, 5048-5049.
271. D. Tobjörk, H. Aarnio, P. Pulkkinen, R. Bollström, A. Määttänen, P. Ihlainen, T. Mäkelä, J. Peltonen, M. Toivakka, H. Tenhu and R. Österbacka, *Thin Solid Films*, 2012, **520**, 2949-2955.
272. S. J. H. Fathima, J. Paul and S. Valiyaveettil, *Small*, 2010, **6**, 2443-2447.
273. S. Marx, M. V. Jose, J. D. Andersen and A. J. Russell, *Biosensors and Bioelectronics*, 2011, **26**, 2981-2986.
274. A. Nouri, P. D. Hodgson and C. e. Wen, *Biomimetic Porous Titanium Scaffolds for Orthopedic and Dental Applications*, 2010.
275. Y. Yamada, Y. C. Li, J. Y. Xiong, T. Banno, P. D. Hodgson and C. E. Wen, in *Eco-Materials Processing and Design X*, eds. H. Kim, J. F. Yang, T. Sekino and S. W. Lee, Trans Tech Publications Ltd, Stafa-Zurich, 2009, pp. 745-748.
276. G. Ryan, A. Pandit and D. P. Apatsidis, *Biomaterials*, 2006, **27**, 2651-2670.
277. C. N. Cornell and J. M. Lane, *Clinical orthopaedics and related research*, 1998, S267-273.
278. G. A. Macheras, P. J. Papagelopoulos, K. Kateros, A. T. Kostakos, D. Baltas and T. S. Karachalios, *Journal of Bone & Joint Surgery, British Volume*, 2006, **88-B**, 304-309.
279. G. He, P. Liu and Q. Tan, *Journal of the mechanical behavior of biomedical materials*, 2012, **5**, 16-31.
280. J. E. Paganessi and J. T. C. Yuan, 2006.
281. Huber, Membrane Bioreactor (MBR), <http://www.huber.de/products/membrane-bioreactor-mbr.html>.

282. S. T. Zhang, Y. B. Qu, Y. H. Liu, F. L. Yang, X. W. Zhang, K. Furukawa and Y. Yamada, *Desalination*, 2005, **177**, 83-93.
283. S. Zhang, F. Yang, Y. Liu, X. Zhang, Y. Yamada and K. Furukawa, *Desalination*, 2006, **194**, 146-155.
284. L. Yihui, N. Kanemaru, M. Nakao, K. Miyasaka and K. Furukawa, *Mem. Fac. Eng. Kumamoto Univ.*, 2005, **49**, 19-3131.
285. Y. H. Xie, T. Zhu, C. H. Xu, T. Nozaki and K. Furukawa, *Water Sci. Technol.*, 2012, **65**, 1102-1108.
286. T. Westermann and T. Melin, *Chemical Engineering and Processing: Process Intensification*, 2009, **48**, 17-28.
287. O. M. Ilinich, F. P. Cuperus, R. W. van Gemert, E. N. Gribov and L. V. Nosova, *Separation and Purification Technology*, 2000, **21**, 55-60.
288. M. E. Ersahin, H. Ozgun, R. K. Dereli, I. Ozturk, K. Roest and J. B. van Lier, *Bioresource Technology*.
289. M. Pera-Titus, M. Fridmann, N. Guilhaume and K. Fiaty, *Journal of Membrane Science*, 2012, **401**, 204-216.
290. J.-O. Kim, J.-T. Jung and J. Chung, *Desalination*, 2007, **202**, 343-350.
291. N. Hengl, A. Mourgues, E. Pomier, M. P. Belleville, D. Paolucci-Jeanjean, J. Sanchez and G. Rios, *Journal of Membrane Science*, 2007, **289**, 169-177.
292. N. Hengl, A. Mourgues, M. P. Belleville, D. Paolucci-Jeanjean and J. Sanchez, *Journal of Membrane Science*, 2010, **355**, 126-132.
293. A. Mourgues, N. Hengl, M. P. Belleville, D. Paolucci-Jeanjean and J. Sanchez, *Journal of Membrane Science*, 2010, **355**, 112-125.
294. E. Pomier, N. Hengl, M.-P. Belleville, D. Paolucci-Jeanjean, J. Sanchez and G. Rios, *Desalination*, 2006, **199**, 185-187.
295. K. Rubow and S. Jha, in *Seventeenth Membrane Technology/Separations Planning Conference*, ed. M. Corporation, Mott Corporation's website, Newton, MA, USA, 1999.
296. I. Kumakiri, J. Hokstad, T. A. Peters, A. G. Melbye and H. Ræder, *Journal of Petroleum Science and Engineering*, 2011, **79**, 37-44.
297. O. M. Ilinich, E. N. Gribov and P. A. Simonov, *Catalysis Today*, 2003, **82**, 49-56.
298. N. Wehbe, N. Guilhaume, K. Fiaty, S. Miachon and J.-A. Dalmon, *Catalysis Today*, 2010, **156**, 208-215.
299. G. Strukul, R. Gavagnin, F. Pinna, E. Modaferri, S. Perathoner, G. Centi, M. Marella and M. Tomaselli, *Catalysis Today*, 2000, **55**, 139-149.
300. R.-H. Kim, S. Lee and J.-O. Kim, *Desalination*, 2005, **177**, 121-132.
301. J. O. Kim, E. B. Shin, W. Bae, S. K. Kim and R. H. Kim, *Desalination*, 2002, **143**, 269-278.